UCRL 9606

University of California

Ernest O. Lawrence Radiation Laboratory

REGENERATION OF θ_1 MESONS IN A THIRTY-INCH PROPANE BUBBLE CHAMBER

Berkeley, California

DISCLAIMER

UCRL-9606
UC-34 Physics
TID-4500 (16th Ed.)

UNIVERSITY OF CALIFORNIA

Lawrence Radiation Laboratory
Berkeley, California

Contract No. W-7405-eng-48

REGENERATION OF θ_1 MESONS IN A THIRTY-INCH PROPANE BUBBLE CHAMBER

Robert H. Good

(Thesis)

July 1961

Printed in USA. Price $1.75. Available from the
Office of Technical Services
U. S. Department of Commerce
Washington 25, D.C.

REGENERATION OF θ_1 MESONS IN A THIRTY-INCH PROPANE BUBBLE CHAMBER

Contents

THIS PAGE

WAS INTENTIONALLY

LEFT BLANK

REGENERATION OF θ_1 MESONS IN A THIRTY-INCH PROPANE BUBBLE CHAMBER

Robert H. Good
(Thesis)

Lawrence Radiation Laboratory
University of California
Berkeley, California

July 1961

ABSTRACT

A beam of θ_2 mesons was produced by passing a beam of 1.1 Bev/c negative pions through a liquid hydrogen target and accepting the neutral reaction products in the forward direction after allowing the θ_1 component to decay. The resultant beam was filtered through four inches of lead and was then observed in a 30-inch propane bubble chamber. Regeneration of the θ_1 component was observed both in lead and iron plates inside the bubble chamber and in the propane itself. About 200 regenerated θ_1 mesons were identified by their characteristic Q-value and decay rate. The observed angular distribution of the θ_1 mesons demonstrated three types of regeneration: incoherent, due to individual nucleons; diffraction, due to all of the nucleons in a nucleus acting coherently; and transmission, due to coherent action of all the matter in the plate as a whole. The Gell-Mann - Pais particle mixture hypothesis is thus further substantiated.

INTRODUCTION

In 1947 the study of neutral K-mesons began with an event observed by Rochester and Butler.[1,2] Upon finding an unusual "fork" of lightly-ionizing, rigid tracks of opposite sign in their magnet cloud chamber, they demonstrated that it was highly improbable that the event was anything other than the decay of a heavy neutral meson. Although the first tentative publication on the pion as such had appeared only a few months previously,[3] and even the mass of the muon was quite uncertain, they managed to infer that the mass of the hypothetical neutral particle was equal to about 1000 electron masses. In succeeding years the two-pion decay mode of the θ^0 meson, with Q-value 217 Mev, was well established by Thompson et al.,[4] and in addition there was found a small admixture of "anomalous" neutral decays of deviant Q-value.[5] In the space of a decade there arose a formidable array[6] of charged and neutral K-mesons:

$$K^+_{\mu 2} \rightarrow \mu^+ + \nu$$
$$K^+_{\pi 2} \rightarrow \pi^+ + \pi^0$$
$$K_{\mu 3} \rightarrow \mu^+ + \nu + \pi^0$$
$$\tau^+ \rightarrow 2\pi^+ + \pi^- \text{ or } \pi^+ + 2\pi^0$$
$$K_{e3} \rightarrow e^+ + \pi^0 + \nu$$

$$\theta^0 \rightarrow \pi^+ + \pi^-$$
$$K^0 \rightarrow e^\pm + \pi^\mp + \nu$$
$$\rightarrow \mu^\pm + \pi^\mp + \nu$$
$$\rightarrow \pi^\pm + \pi^\mp + \pi^0$$

All of these K mesons appeared to have the same mass.

With substantiation[7] of Lee and Yang's suggestion[8] that parity need not be conserved in weak interactions, it became possible to simplify the picture greatly by considering the entire K-meson complex as just one isotopic-spin doublet, with antiparticles:

Particle -- K^+, $\theta^0(K^0)$

Antiparticle -- $K^-(\overline{K^+})$, $\overline{\theta^0}(\overline{K^0})$.

Agreement of the results of this experiment and others[9,10] with those predicted on the basis of the assumption that K^+ and K^0 are an isotopic doublet constitutes evidence for this assumption and against opposed schemes such as that of Pais.[11]

The K^+ and θ^0 mesons were assigned a strangeness[12] of +1; the θ^0 appeared to differ from its antiparticle only in strangeness. In 1955 Gell-Mann and Pais pointed out[13] that consequently the θ^0 and $\overline{\theta^0}$ mesons may be expected to be mixed by the intermediate two-pion state:

$$\theta^0 \longleftrightarrow \pi^+ + \pi^- \longleftrightarrow \overline{\theta^0}$$

Strangeness is not conserved in this weak interaction. An initially pure θ^0 beam should contain appreciable amounts of $\overline{\theta^0}$ component after a time comparable to the lifetime for two-pion decay of the θ^0 meson because of the above-mentioned mixing. This led Gell-Mann and Pais to predict two-component properties for the neutral K meson. As the decay product $\pi^+ + \pi^-$ is an eigenstate of CP, whereas the θ^0 and $\overline{\theta^0}$ are not (they have different strangeness), it is reasonable to postulate the existence of θ_1 and θ_2 eigenstates of CP such that

$$\theta_1 = \frac{\theta^0 + \overline{\theta^0}}{\sqrt{2}} \tag{1}$$

$$\theta_2 = \frac{\theta^0 - \overline{\theta^0}}{i\sqrt{2}} \tag{2}$$

from which it follows that

$$\theta^0 = \frac{\theta_1 + i\theta_2}{\sqrt{2}} \tag{3}$$

$$\overline{\theta^0} = \frac{\theta_1 - i\theta_2}{\sqrt{2}} \tag{4}$$

As CP is presumably conserved in the weak interactions leading to decay, one may assign to θ_1 alone the neutral K meson decays that are even under CP:

$$\left.\begin{aligned} \theta_1 &\rightarrow \pi^+ + \pi^- \\ &\rightarrow 2\pi^0 \end{aligned}\right\} \text{ fast, } 10^{-10} \text{ second}$$

and to θ_2 alone those that are odd:

$$\theta_2 \rightarrow 3\pi^0 \qquad \text{slow, } 10^{-7} \text{ seconds.}$$

In addition, both θ_1 and θ_2 mesons may presumably undergo leptonic decays, and decays to the final state $\pi^+\pi^-\pi^0$ at rates comparable to those for $3\pi^0$ decays[14]. Existence of such a long-lived neutral θ meson was established by Lande et al.[15]

As previously, one assigns to θ^0 those interactions which involve positive strangeness:

$$\theta^0 + p \rightarrow K^+ + n$$

$$\pi^- + p \rightarrow \Lambda^0 + \theta^0$$

and to $\overline{\theta^0}$ those interactions which involve negative strangeness:

$$\overline{\theta^0} + n \rightarrow K^- + p$$

$$\overline{\theta^0} + p \rightarrow \Lambda^0 + \pi^+.$$

According to this theoretical picture, θ^0 and $\overline{\theta^0}$ mesons may each decay with equal probability by the θ_1 or θ_2 modes, and θ_1 and θ_2 mesons may interact with equal probability in the θ^0 and $\overline{\theta^0}$ modes. The former prediction has been confirmed by Eisler et al.[16], who observe, using a propane bubble chamber, that indeed one-half of the θ^0's produced in the

reaction

$$\pi^- + p \rightarrow \Lambda^\circ + \theta^\circ$$

are long-lived. The prediction of equal θ_2 interaction in eigenstates of strangeness plus one and minus one is supported by several investigations.[10,17,18]

Lee and Yang[19] have pointed out that, in those cases in which $p + \bar{p} \rightarrow \theta^\circ + \overline{\theta^\circ}$, the $\theta^\circ\ \overline{\theta^\circ}$ system may be expected to be in an odd CP state, and consequently, if CP is assumed to be conserved, the probability of simultaneously observing both neutral θ's to decay as θ_1's, or to interact as $\overline{\theta^\circ}$'s, is zero. No experimental study of this phenomenon has as yet been reported.

Regeneration of θ_1 mesons is another consequence of the theory and it may be observed experimentally as follows: A θ° beam devoid of $\overline{\theta^\circ}$ component may be produced by bombarding protons with negative pions at an energy above the threshold for the reactions producing θ° mesons but below that for reactions producing $\overline{\theta^\circ}$ mesons. As may be seen from the accompanying table of fundamental particles, Table I,[20] a 1.1 Bev/c π^- meson beam impinging on a hydrogen target cannot, by any known reaction, produce $\overline{\theta^\circ}$ mesons when mass and strangeness are conserved; yet it can produce θ° mesons by the following reactions:

$$\pi^- + p \rightarrow \Lambda^\circ + \theta^\circ \qquad 0.80\ mb$$

$$\rightarrow \Sigma^\circ + \theta^\circ \qquad 0.34\ mb$$

$$\pi^- + n \rightarrow \Sigma^- + \theta^\circ \qquad .3?\ mb$$

The Λ° and Σ° hyperons decay quickly, so that the presence of particles of negative strangeness more than a few centimeters from the source of

TABLE I

Particle	Mass (Mev)	Mean Life (sec)
$\pi^{\pm}$	139.59	2.55×10^{-8}
π^{o}	135.00	2.2×10^{-16}
$K^{\pm}$	493.9	1.22×10^{-8}
K_1^{o}	497.8	1.00×10^{-10}
K_2^{o}	497.8	6.1×10^{-8}
p	938.21	∞
n	939.51	1.01×10^{3}
Λ	1115.4	2.50×10^{-10}
Σ^{+}	1189.4	$.81 \times 10^{-10}$
Σ^{-}	1196.0	1.6×10^{-10}
Σ^{o}	1192	$.1 \times 10^{-10}$
Ξ^{-}	1318	1.3×10^{-10}
Ξ^{o}	1311	1.5×10^{-10}

the beam must be explained on the basis of the particle mixture hypothesis. When the θ^o beam has traveled several θ_1 lifetimes, the θ_1 component of the beam (see Eq. 3) has for the most part decayed away, while the long-lived θ_2 component remains almost undiminished. By Eq. 2 the resultant θ_2 beam contains $\overline{\theta^o}$ mesons; they may be detected in the presence of matter by observing interactions involving negative strangeness, such as production of Λ^o hyperons according to the reaction

$$\overline{\theta^o} + p \rightarrow \Lambda^o + \pi^+$$

Detection of the $\overline{\theta^o}$ component in this way has furnished another means of verifying the particle mixture hypothesis, both in propane and hydrogen bubble chambers[17] and in emulsion.[10,18] If now the θ_2 beam is passed through an absorber, as suggested by Pais and Piccioni,[21] the $\overline{\theta^o}$ component is absorbed preferentially because it can produce hyperons, by virtue of its negative strangeness, whereas the θ^o component cannot. The relative enhancement in magnitude, and shift in relative phase, of θ^o with respect to $\overline{\theta^o}$ in Eq. 2 results in an increase in θ_1, i.e., in "regeneration" of the θ_1 component of the beam. Detection of this component by observing its characteristic decay, first accomplished in the present experiment, constitutes another method of verifying the particle mixture hypothesis.

Interaction of θ_2 mesons with individual nucleons yields a diffuse angular distribution of θ_1 mesons which is characteristic of K-nucleon scattering and hence is not a crucial consequence of the particle mixture hypothesis. On the other hand, this theory predicts that θ_1 mesons may also be regenerated by means of diffraction[22] and refraction about nuclei

as a whole, with all of the matter of the nucleus contributing coherently to the regeneration. An identity change (as θ_2 to θ_1) during diffraction can only result from the fact that the initial beam consists of a mixture or superposition of several components which interact differently with nuclei and which are consequently diffracted differently by nuclei. Thus this phenomenon contrasts with, for example, photo-production of π^0 mesons, or π^- charge exchange, in which the resultant π^0 beam displays no such coherence in the forward direction. As the $\overline{\theta^0}$ interacts more strongly than the θ^0 with nuclear matter, it is diffracted more strongly; the $\overline{\theta^0}$ is, so to speak, separated from the θ^0, so that its θ_1 component may be observed. These diffraction-regenerated θ_1's show the sharply peaked angular distribution which is characteristic of diffraction about nuclei. The observation of such a peaked angular distribution in the present experiment constitutes the first experimental demonstration that particles may change their identity by means of a diffraction interaction. This is a striking confirmation of the particle mixture hypothesis.

It has been suggested[13,23] that the masses of the θ_1 and θ_2 mesons differ by an amount $m = \hbar\delta/c^2 t_1$, where t_1 is the lifetime of the shorter-lived (θ_1) meson and δ is a dimensionless quantity of the order of unity. This leads to an oscillatory term in the wave equation of a θ^0 or $\overline{\theta^0}$ beam due to interference between the θ_1 and θ_2 components:

Number of $\overline{\theta^0}$ in θ^0 incident beam = $1 + \exp(-t/t_1) - 2\exp(-t/2t_1)\cos(t/t_1\delta)$

for $t_2 \gg t_1$

and $t_2 \gg t$,

where t_1 and t_2 are the lifetimes of the θ_1 and θ_2 mesons, respectively. This corresponds to an alternate disappearance and reappearance of the θ^o and $\overline{\theta^o}$ components of the beam. The oscillation is damped down, by the decay of the θ_1 component, to an equilibrium state which in the absence of matter consists of equal amounts of θ^o and $\overline{\theta^o}$ components with a phase relationship corresponding to the θ_2 meson. Oscillations in the $\overline{\theta^o}$ flux may be monitored by means of reactions involving negative strangeness[24,25], such as reaction (3). Boldt et al.[25] have observed this effect, using 1.5 Bev/c pions in the MIT multiplate cloud chamber; the 12 events they analyzed, along with other data, suggested a most probable value of δ of one. Similarly, Birge et al.[26] have investigated the production of hyperons following charge exchange of K^+ mesons in a 30-inch propane bubble chamber; they have found a preliminary value of $\delta = 1.5 \pm .5$ after analyzing about 1/4 of their data (65 events out of about 250).

In the present experimental arrangement, however, the number of θ_1's produced is less than 1% of the number of θ_2's transmitted, so that oscillations in the $\overline{\theta^o}$ flux are small, and variations in the frequency of hyperon production in the propane as a function of distance from the absorber are not detectable.

Trieman and Sachs[27] have suggested that observation of oscillations in the ratio of θ_2 decays $\frac{e^+\pi^-\nu}{e^-\pi^+\nu}$ with distance from the origin of the θ^o's would yield information on the θ_1-θ_2 mass difference, and Biswas has pointed out[28] that even the sign of the mass difference may be obtained in this way. Similarly, Trieman and Weinberg[29,30] have suggested that a study of the change in momentum distribution of $\pi^+\pi^-\pi^o$

decays with time could yield information both on the mass difference and on the $\Delta I = \frac{1}{2}$ rule. Such variations are again small in the present experiment, and, in addition, the number of identifiable θ_2 decays is too small for analysis of this kind.

Another method of detection of the θ_1-θ_2 mass difference has been worked out in detail by M. Good.[30,31] When $\overline{\theta^0}$ mesons are removed preferentially by nuclear interactions, giving diffraction-regenerated θ_1's, as noted above, there remains an excess of undisturbed θ^0's continuing in the forward direction. The θ_1 component of these transmitted θ^0's may then be observed with a very sharply peaked forward angular distribution whose width is due only to the size of the source of the original θ_2 beam and to the errors of measurement of the θ_1 decay products. All of the matter in the plate acts coherently so that the effect is that of diffraction by the plate as a whole. Each nucleus produces a forward θ_1 wave which is coherent with those produced by the other nuclei. The θ_1 and θ_2 waves have frequencies which differ by an amount corresponding to their mass difference; consequently, the phase of the transmission-regenerated θ_1 wave as it leaves the plate depends on where it originated in the plate, and cancellation between the θ_1 wave amplitudes from various depths in the plate will occur to a degree determined by the mass difference. If the mass difference is zero, then there is no such cancellation and a strong forward θ_1 component should be observed. Comparison of the transmission-regenerated component, which is thus sensitive to the θ_1-θ_2 mass difference, with the diffrac-

tion-regenerated component, which is relatively insensitive to it, has yielded a mass difference of $\delta = .77$.[32]

In the Θ_2 to Θ_1 transformation, the total energy is expected to remain practically constant while the mass changes. This is because the nucleus, being heavy, absorbs very little energy with respect to the momentum transfer. If we write for the nucleus

$$E^2 = P^2 + M^2$$

then we have

$$dE = \frac{P}{E}\, dP \ll dP$$

as the rest mass of the nucleus is very large and does not change. Thus in the wave equations we may set

$$\omega_2 = \omega_1 \quad \text{(total energy conservation)}.$$

Other choices are conceivable, such as:

$$k_2 = k_1 \quad \text{(momentum conservation)}$$

$$\beta_2 = \beta_1 \quad \text{(velocity conservation)}.$$

The last is attractive because of its invariance to coordinate transformation. However, the physical, observable consequences are the same for these three possible assumptions, and the first is chosen for the reason given above.

The choice

$$M_2 = M_1$$

would also be attractive, not only because of its invariance with respect to coordinate transformation, but also because the concept of a change in rest mass (not to mention CP characteristics) of a particle during a diffraction interaction has been foreign to physical theory.[33]

However, the change of mass during diffraction is not forbidden by any theoretical consideration. On the other hand, its observation is limited to cases involving very small mass changes, for the following reason. If the θ meson keeps the same total energy during its transformation, then we can write

$$dP = -\frac{M}{P}\,dM = -\frac{dM}{\beta\gamma} = 10^{-5}\ \text{ev/c}$$

This is the momentum that must be transferred to the nuclei by the θ meson. For regeneration in the forward direction, there is no other momentum transfer. Clearly no individual nucleon in a nucleus can absorb so little momentum because the nuclear levels are relatively widely spaced. And, in fact, the nuclei in the crystal lattice are also incapable of doing so. In order to have level spacings corresponding to 10^{-5} ev/c, particles must be quantized in a region on the order of

$$x = \frac{\lambda\!\!\!^{-}}{10^{-5}} \approx 1\ \text{cm.}$$

Thus we see that a region of the plate on the order of 1 cm can absorb the momentum change; so we expect experimentally to see coherence effects due to coherent action of all the atoms in a 1 cm region of the plate. If, on the other hand, the mass difference were zero, the whole plate could contribute coherently. And if the mass difference were on the order of several Mev, then no more than one nucleus could participate in the forward coherent regeneration of θ_1's.

This argument sets an upper limit on the size of the object all of whose parts can contribute coherently to regeneration. It does not

set a lower limit because all nuclei, or nucleons in the nuclei, may regenerate Θ_1's incoherently from each other by scattering through a wide angle, for which the momentum transfer is large compared to that which is due to the mass difference.

EXPERIMENTAL PROCEDURE

Fig. 1 shows the experimental arrangement. The circulating beam of protons, having an energy of 5.3 Bev, impinged upon a copper target inside the Bevatron. The negative particles emerging from the target in the forward direction, consisting mainly of pions, left the Bevatron and entered a chain of bending and focusing magnets designed to select those particles having a momentum of 1.1 Bev/c $\pm$ 5% and to pass them through a liquid hydrogen target. This beam is shown schematically in Fig. 2, with the central momentum trajectory straightened out for clarity, so that only particles which deviate from the central momentum (1.1 Bev/c) show any deflection in the bending magnets.

The behavior of the pions under the influence of the Bevatron's magnetic field was computed by means of an IBM 650 computer programmed for that purpose;[34] the positions and directions of the trajectories thus obtained were calculated for the point at which the pions enter the first quadrupole magnet, and from these were computed the horizontal and vertical positions and sizes of a virtual image of the target which was then introduced as shown in Fig. 2 to replace the relatively-complicated Bevatron fringing field and target. Using an electrical analog computer,[35] trajectories of the pions were calculated from the virtual target to a more or less arbitrary point safely beyond the propane bubble chamber. In designing the beam particular care was exercised to minimize the amount of scraping of the pion beam against the sides of magnets, which would have resulted in contamination of the beam with unwanted charged and neutral particles.

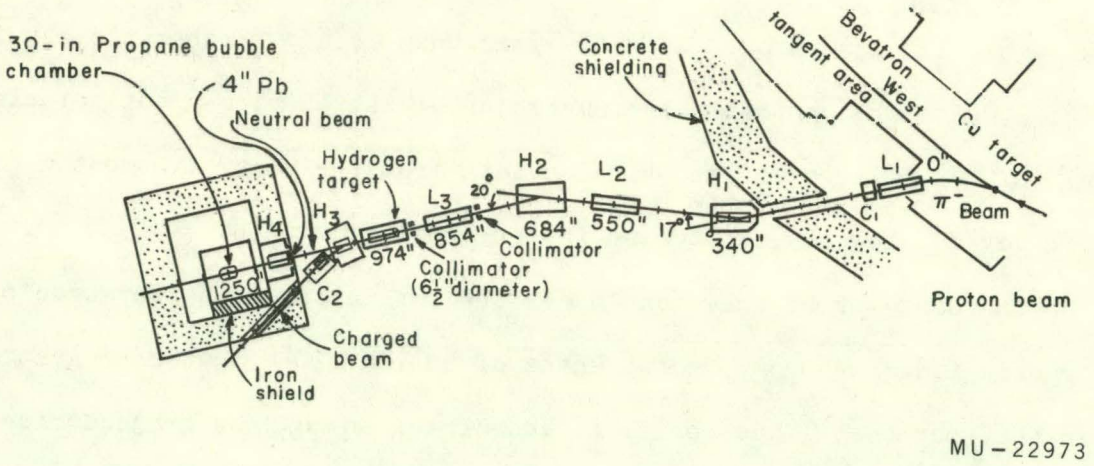

Fig. 1. Experimental arrangement. L_1, L_2, and L_3 are 8-inch quadrupole focusing magnets; H_1, H_2, H_3, H_4, C_1, and C_2 are bending magnets.

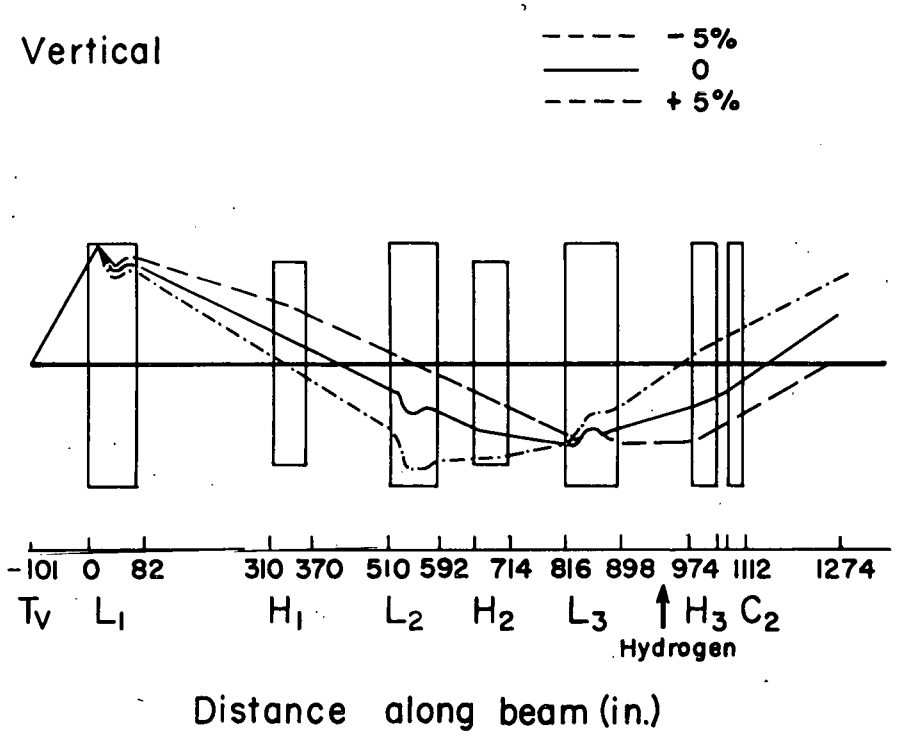

Fig. 2A. Schematic diagram of beam. Vertical plane, T_V is the virtual target in the vertical plane.

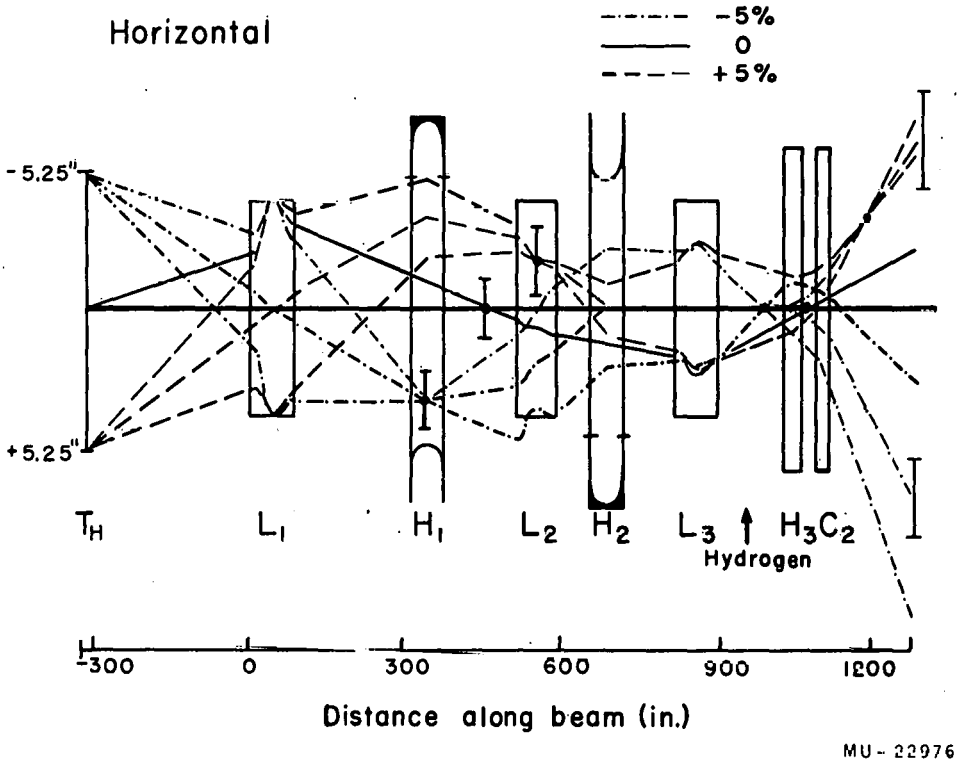

Fig. 2B. Schematic diagram of beam. Horizontal plane. T_H is the virtual target in the horizontal plane.

Field values obtained from the analog computation were refined by means of wire-orbit procedures, and received a final adjustment, using scintillation counters, when a pion beam became available from the Bevatron.

The first quadrupole, L_1, focused the Bevatron target on the second quadrupole, L_2. The first C magnet, C_1, was adjusted to a small field value in order to maximize the pion beam. The first analyzing magnet, H_1, assisted by the field of the Bevatron, produced a dispersion between H_1 and the second quadrupole, making possible momentum determination at this point. The second quadrupole focused the first quadrupole through the third onto the hydrogen target. The second analyzing magnet, H_2, eliminated the dispersion so that the beam striking the hydrogen target was nearly achromatic. The third quadrupole, L_3, focused the second quadrupole at a point somewhat beyond the propane chamber in order to minimize spreading and possible scattering of the beam after it left the hydrogen target.

Upon entering the 5-foot liquid hydrogen target the 1.1 Bev/c pions created Θ^0 mesons by means of the reactions

$$\pi^- + p \rightarrow \Lambda^0 + \Theta^0, \qquad \sigma = .80 \text{ mb}$$

$$\pi^- + p \rightarrow \Sigma^0 + \Theta^0, \qquad \sigma = .34 \text{ mb}$$

In addition, neutrons and photons were produced by the reactions:

$$\left.\begin{array}{l} \pi^- + p \rightarrow \pi^0 + n, \\ \qquad\qquad \pi^0 + p + \pi^-, \text{ etc.} \end{array}\right\} \quad \begin{array}{l} \sim 15 \text{ mb for } \pi^0 \\ \sim 15 \text{ mb for } n \end{array}$$

$$\pi^0 \rightarrow 2\gamma$$

The beam and secondary charged particles emanating from the hydrogen target were swept away by the magnets H_3 and C_2. The neutral reaction products in the forward direction encountered a 4-inch lead window which reduced the photon component by a large factor while reducing the neutron and θ_2 components by about half. The bending magnet H_4 swept away the conversion electrons.

The resulting neutral beam passed into the 30-inch propane bubble chamber.[36] The chamber was operated at a repetition rate of twelve per minute in a magnetic field of 13.4 kilogauss. 206,000 Bevatron pulses were photographed stereoscopically between April 30 and May 21, 1959. A metal plate was placed in the propane chamber for the regeneration of θ_1 mesons. For the first 123,000 pictures this plate consisted of two parts, one lead and one stainless steel, each 1½-inches thick, as shown in Fig. 3. For the rest of the pictures, up to 206,000, this plate was replaced with a stainless-steel plate 6-inches thick which was intended to enhance the transmission-regeneration effect. Fig. 4 shows view 1 of picture number 205,516; a θ_1 meson decay is visible near the center of the chamber.

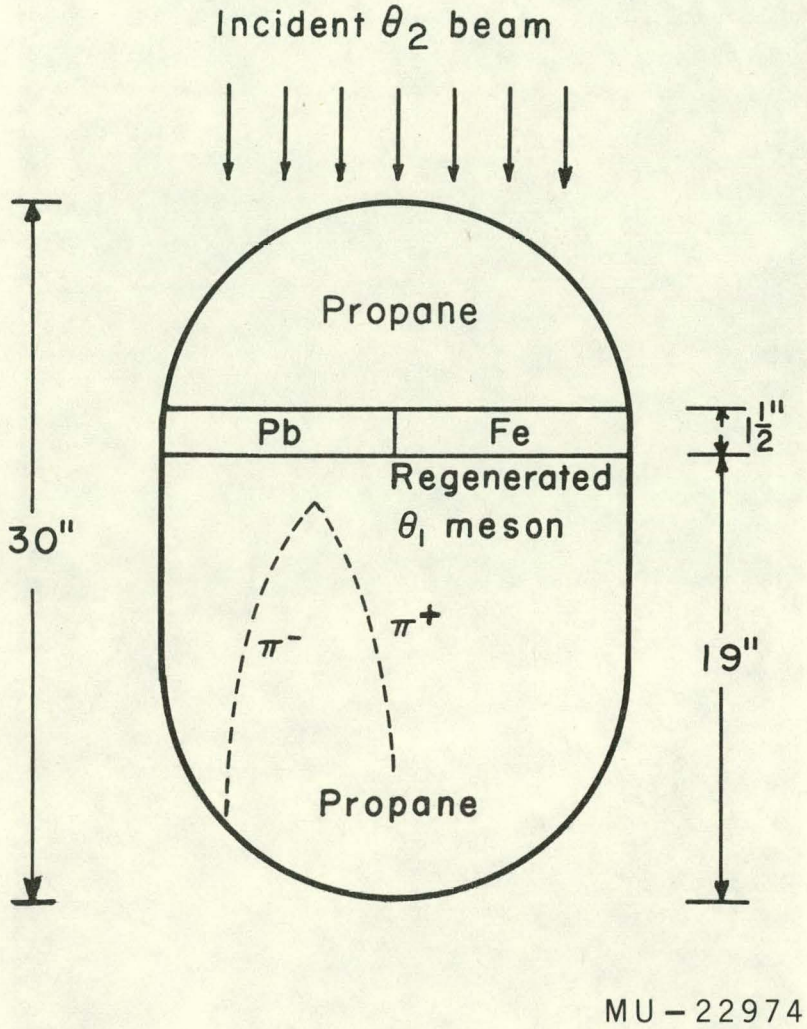

Fig. 3. Diagram of bubble chamber showing 1-1/2-inch plates and θ_1 decay.

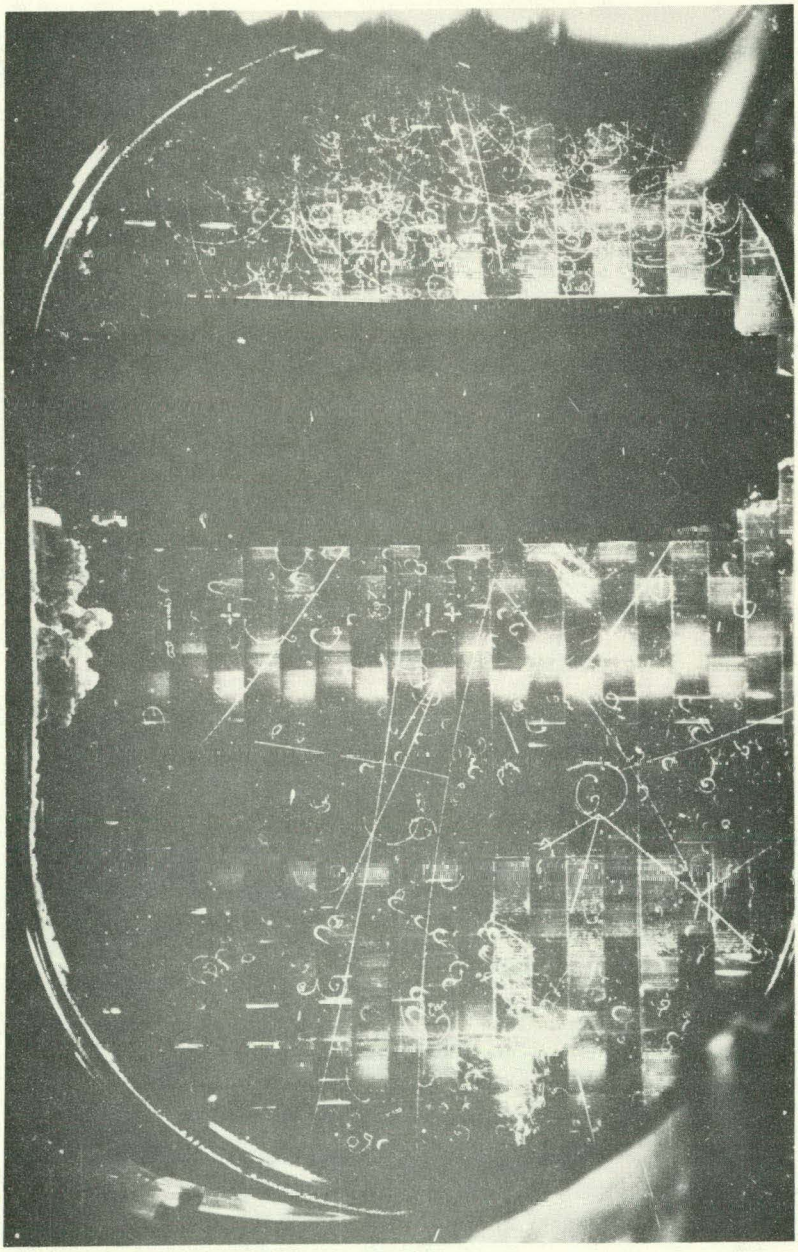

ZN-2949

Fig. 4. Photograph of event number 205,516, showing 6-inch plate and θ_1 decay.

SCANNING OF FILM

The 206,000 pictures were scanned by means of over-head stereo projectors which projected the two full-size stereo views of the chamber independently on a white surface. The film was scanned for all V^o-type events which were measurable and were pointed more or less toward the metal plate in the bubble chamber. Events showing any perceptible blob at the origin, which could be due to a recoil nucleus, were rejected. Scanning efficiency for Θ_1 mesons was found to be about 75%, by means of careful rescans and comparisons of events found. (Efficiency for detection of lambda-type events, on the other hand, was somewhat greater, about 85%, presumably because the positive track of a lambda is generally heavily-ionizing at these energies and thus is easier to detect than the minimum-ionizing pion tracks of a Θ_1.) About 70% of the film was rescanned, so the overall efficiency for detecting Θ_1 mesons is taken to be about 89%.

As a background check, 48% of the film was scanned also for pseudo-V^o events having a third prong which was an identifiable proton between 2 mm and 8 cm long.

MEASUREMENT AND CALCULATION

The events were measured either on stage microscopes, with digitizers which automatically punched IBM cards, or on a "Frankenstein" automatic measuring and card-punching machine. Either machine measured the position of the origin of an event and of several points along each track, after which these data were sent to the IBM 704 for computation of the characteristics of the event.

The data obtained from the measuring devices were processed by IBM 704 computers. The first program, called Fog 4, calculated the characteristics of each track independently, and the second, called Cloudy, calculated quantities involving the relative position and monenta of the two tracks involved in each event. Two complete calculations were made for each event, one on the assumption that it was a lambda decay (i.e., that the positive prong was a proton and the negative prong was a pion) and the other on the assumption that it was a theta (both prongs were pions). All relevant quantities for each event appeared on a single sheet of output.

EDITING

About 15,000 events were found by the scanners, of which all but 1200 were discarded after careful examination by the experimenters. An event was discarded if its positive prong could be identified as a proton (either by ionization or by the fact of its stopping in the liquid of the chamber), if it was of such poor quality that it could not be accurately measured (about 50% error in momentum), if it had a blob at the vertex in both stereoscopic views, if it appeared to be merely a proton or meson scatter, or electron-positron pair (zero opening angle), or if it pointed backwards (away from the plate). Events with identifiable electrons or muons were not included in the data of this paper. Whenever there was any question as to whether an event satisfied the above criteria, the event was rejected.

Pictures varied greatly in bubble density and consequently in ease of proton identification; in some portions of the experiment, tracks were so heavy that electrons could not be distinguished from stopping protons on the basis of bubble density, while in other portions bubble density was so low that electrons were barely detectable. Even in the best portions of film it was usually difficult to distinguish protons from positive pions at momenta much above 600 Mev/c; consequently all events having a positive prong whose momentum exceeded 600 Mev/c were discarded. This removed about 20% of the Θ_1 decays present and altered the momentum distribution of the remaining Θ_1's. This effect has been included in the calculations of the expected Θ_1 momentum distribution, and it cannot affect any of the conclusions drawn in this paper. About 100 times as many background events as Θ_1 decays were removed by this criterion; almost all of these events would of course have been removed

by other criteria, particularly the requirement that the positive prong definitely not be a proton.

Twenty-two events having an error in Q-value which was at least half of the Q-value were discarded.

The accepted events having a Q-value between 170 and 280 Mev were carefully re-examined for possible origins in the propane within ten centimeters of the event. Twenty such origins were identified. The corresponding events were then removed from the data used in studying regeneration in the metal plates and were examined in a separate section of this paper dealing with regeneration in propane.

RESULTS AND DISCUSSION

A. Regeneration in Lead and Iron Plates.

Figure 5 shows the Q-value distribution for all 1159 events meeting the acceptance criteria (see Editing, above). The peak of the curve at the characteristic 218-Mev Q-value indicates that large numbers of θ_1 mesons are indeed present and that therefore regeneration of θ_1 mesons is being observed.

It is possible that some of the events in the graph of Fig. 5 are in reality nuclear interactions having two visible charged prongs and one or more neutrons or other uncharged, invisible prongs. Some indication of the number of such events present may be obtained by observing the frequency of occurrence and other characteristics of nuclear events which resemble θ_1 meson decays except in that they have a third prong which is a relatively slow proton. Consequently about half of the film was scanned for events having a third prong which was an identifiable proton between 2 mm and 8 cm long. Forty-nine such events were found, indicating that corresponding cases in which the third prong is a neutron should not contribute much more than 10% to the background. In Fig. 6 the Q-values of such events are plotted. Complete absence of a peak at 218 Mev further substantiates the supposition that the peak of Fig. 5 is due essentially to θ_1 mesons.

To facilitate further study of the regenerated θ_1 mesons and reduce the background of θ_2 mesons and neutron stars, three more stringent acceptance criteria have been employed, namely:

(Q) The Q-value of the event must be between 170 and 280 Mev.

(P) The momentum of the presumed θ_1 meson must be above 500 Mev/c.

(T) The event must occur within two θ_1 mean lives of the plate.

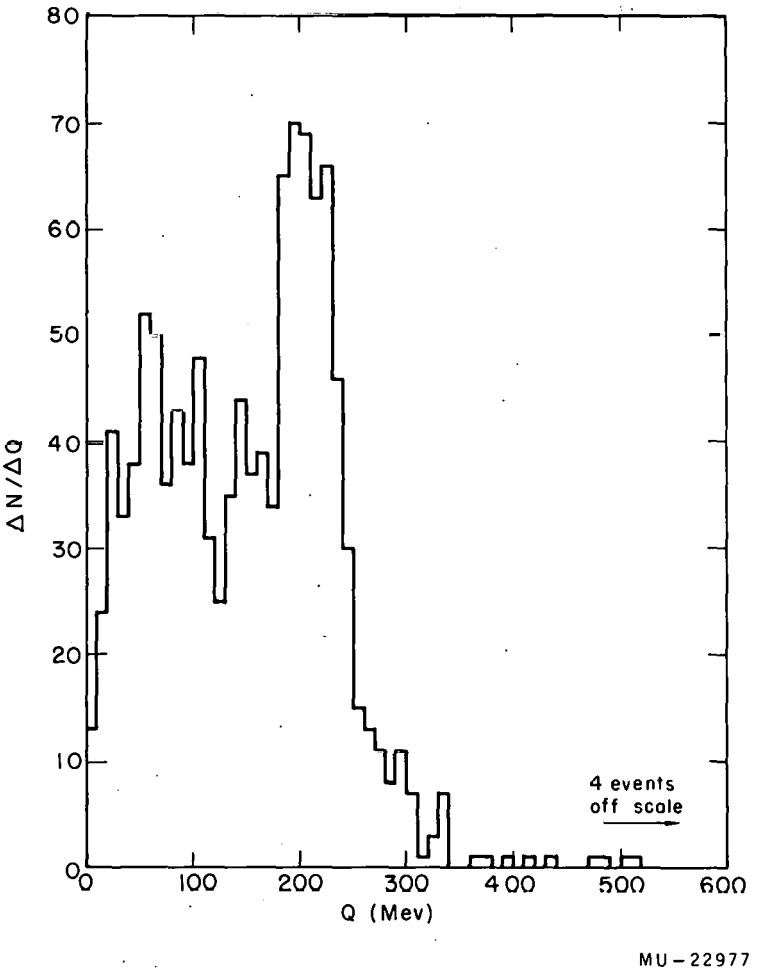

Fig. 5. Q-value distribution of 1159 accepted events.

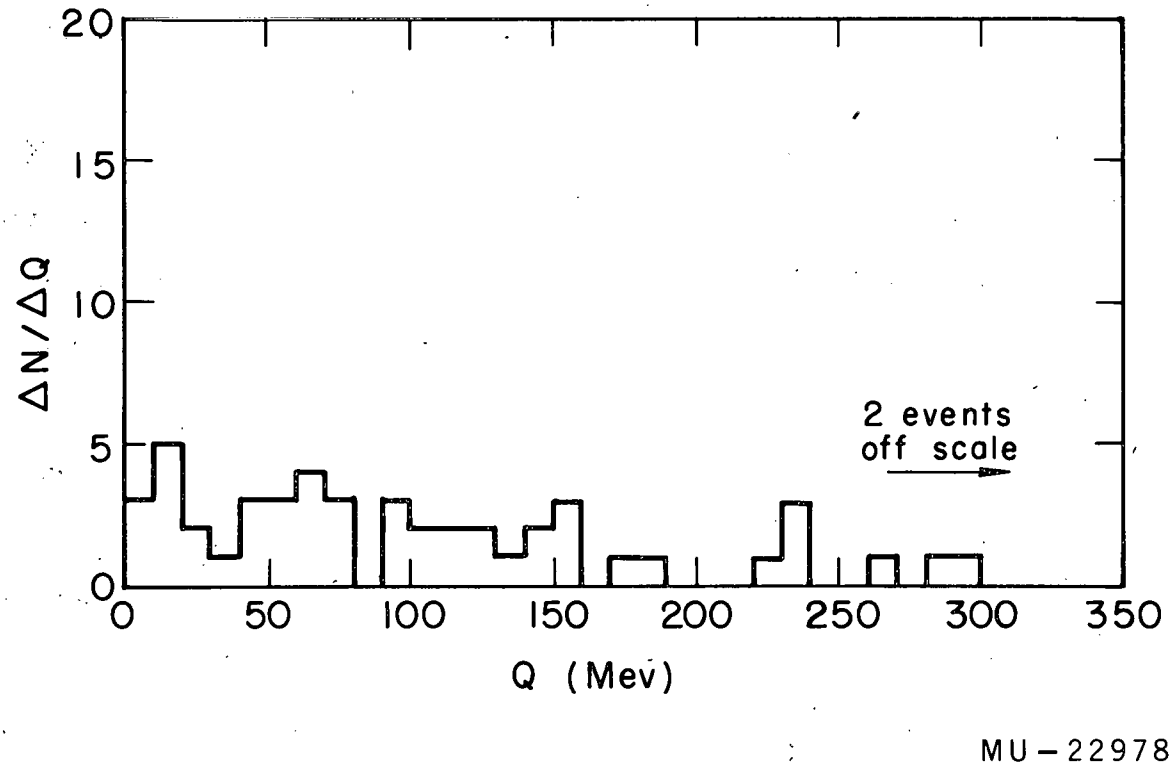

Fig. 6. Q-value distribution of three-prong events which are otherwise acceptable.

Hereafter these will be called the Q, P, and T criteria.

In Figs. 7 through 18 the Q-value distribution of the 1159 events of Fig. 5 is broken up into its component parts by lifetime and momentum for the 1½-inch and 6-inch plates separately. The peak at 218 Mev is apparent only for events satisfying the P and T criteria (Figs. 7 and 13), indicating that these criteria are indeed effective in removing unwanted background events.

Absence of a Q-value peak in Figs. 8, 9, 14, and 15, which satisfy the P criterion but not the T criterion, indicates that θ_1 regeneration in the propane of the bubble chamber is a relatively small effect in the present experiment, and that regeneration is occurring primarily in the metal plates.

Figure 19 shows the momentum distribution of events satisfying the Q and T criteria, along with a theoretical momentum distribution calculated for the conditions of this experiment[32]. (The calculation was based on the assumption that the incident pion beam momentum distribution was a Gaussian centered about 1.1 Bev/c and with a width of 0.055 Bev/c. As this distribution was never measured, the calculated θ_1 momentum distribution may deviate somewhat from the actual one, but the central momentum should be fairly accurate. The experimental distribution appears to match the theoretically expected one. The P criterion should remove about 10.1% of the θ_1 mesons, according to this figure.

Figure 20 shows the lifetime distribution of events meeting the Q and P criteria, along with a θ_1 decay curve. The lifetime of the QP events is evidently equal to the θ_1 lifetime of 1.0×10^{-10} seconds, which further verifies that θ_1 regeneration is occurring. The T criterion

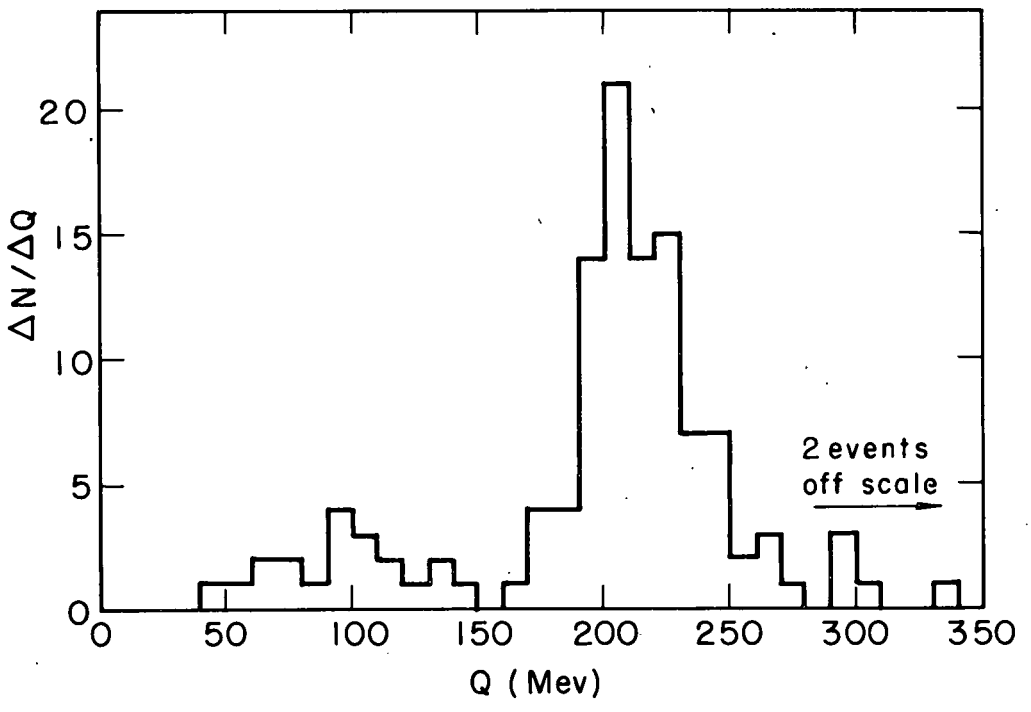

Fig. 7. Q-value distribution of events from the 1-1/2-inch plate having P > 500 Mev/c and 0 < t < 2 mean lives.

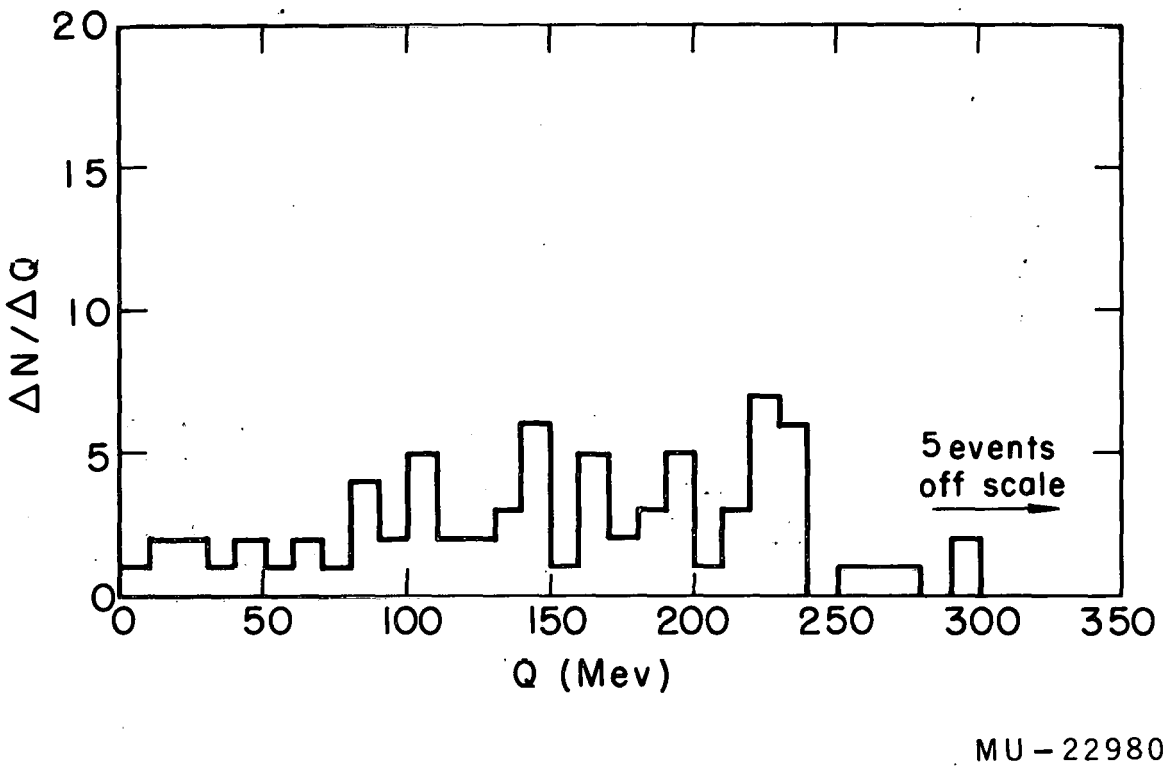

Fig. 8. Q-value distribution of events from the 1-1/2-inch plate having P > 500 Mev/c and 2 < t < 4 mean lives.

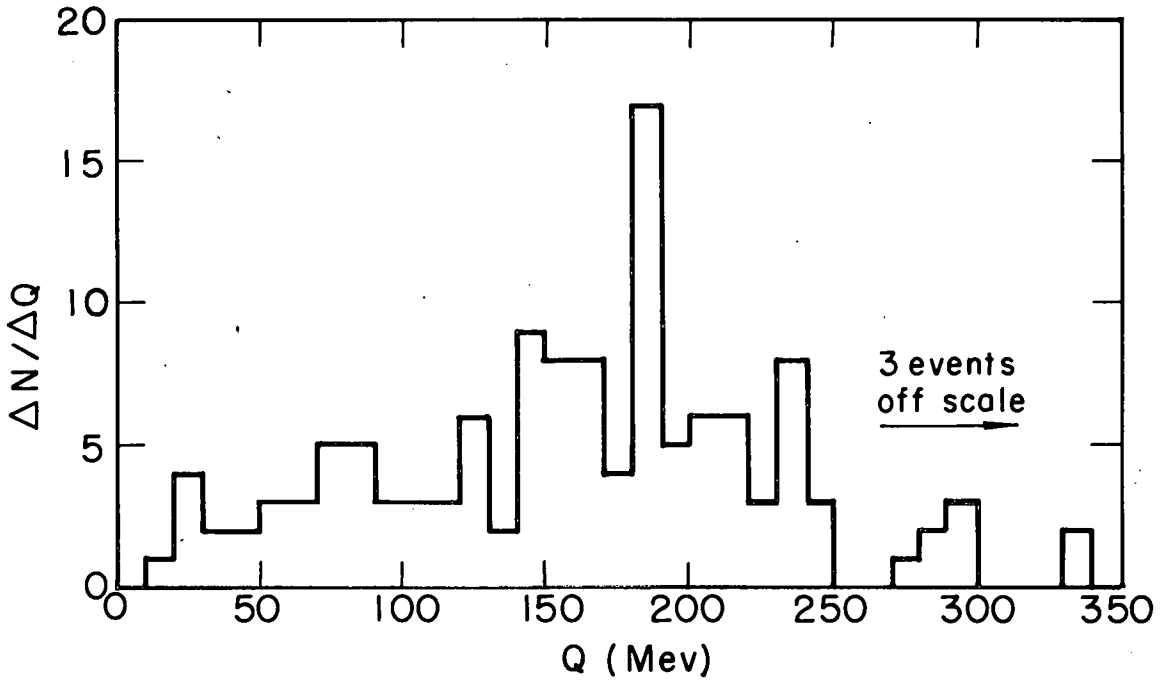

MU-22981

Fig. 9. Q-value distribution of events from the 1-1/2-inch plate having P > 500 Mev/c and 4 < t < 00 mean lives.

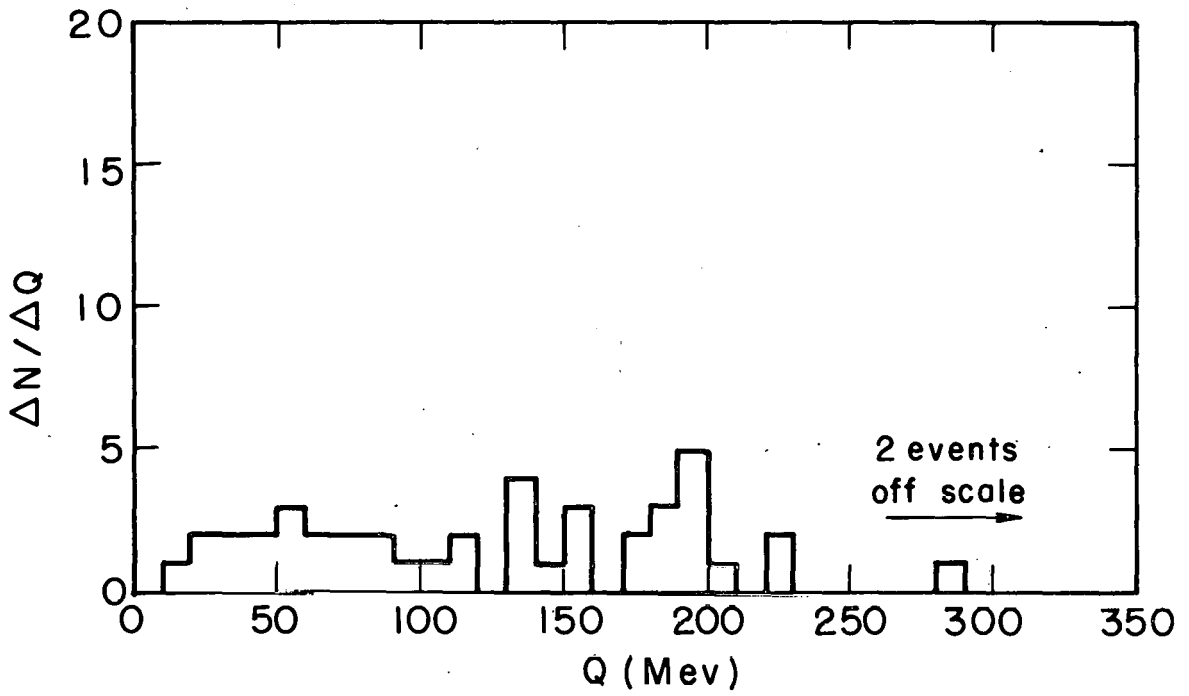

Fig. 10. Q-value distribution of events from the 1-1/2-inch plate having P < 500 Mev/c and 0 < t < 2 mean lives.

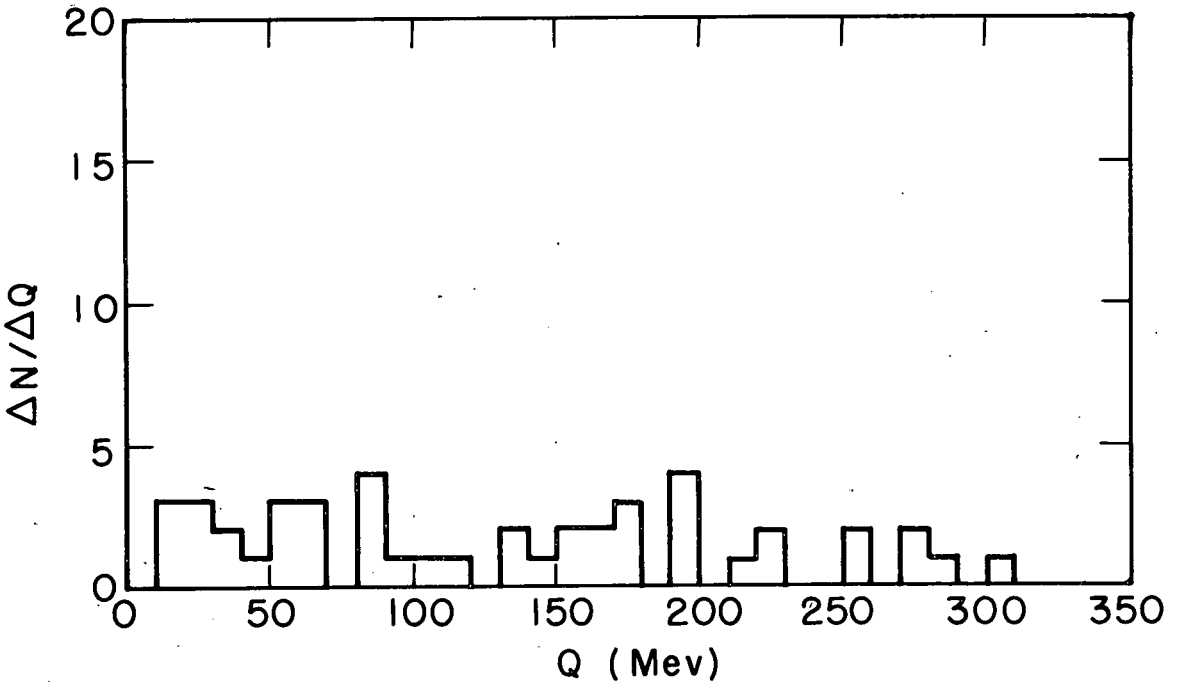

Fig. 11. Q-value distribution of events from the 1-1/2-inch plate having P < 500 Mev/c and 2 < t < 4 mean lives.

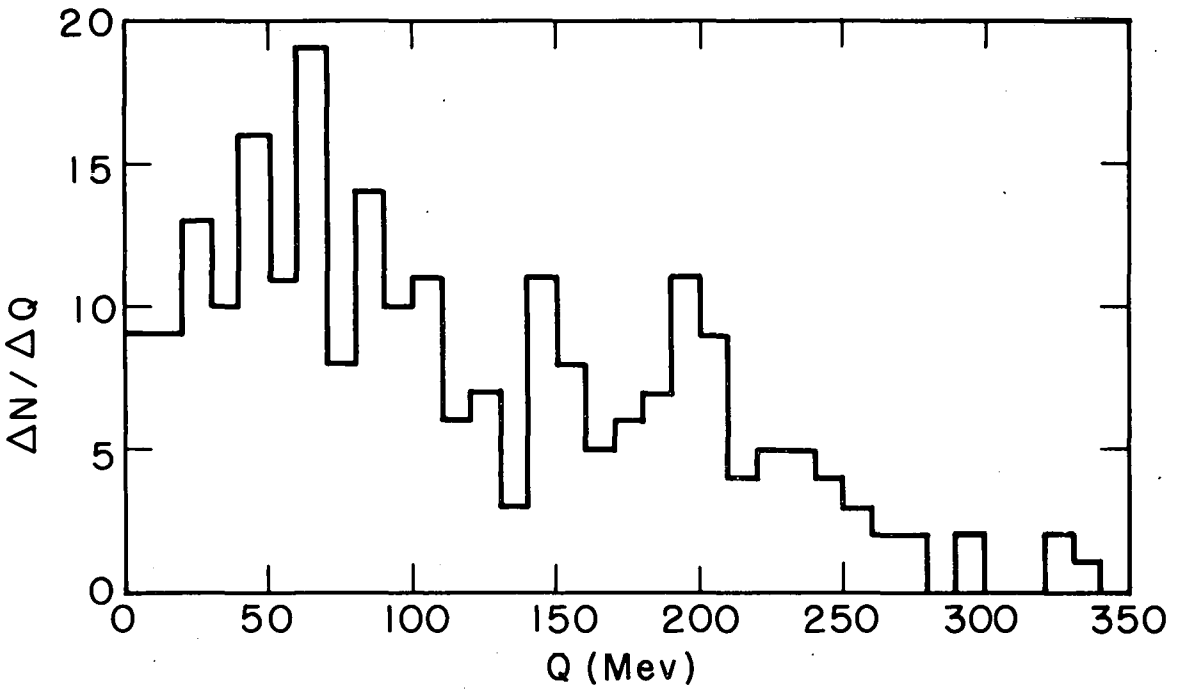

Fig. 12. Q-value distribution of events from the 1-1/2-inch plate having P < 500 Mev/c and 4 < t < 00 mean lives.

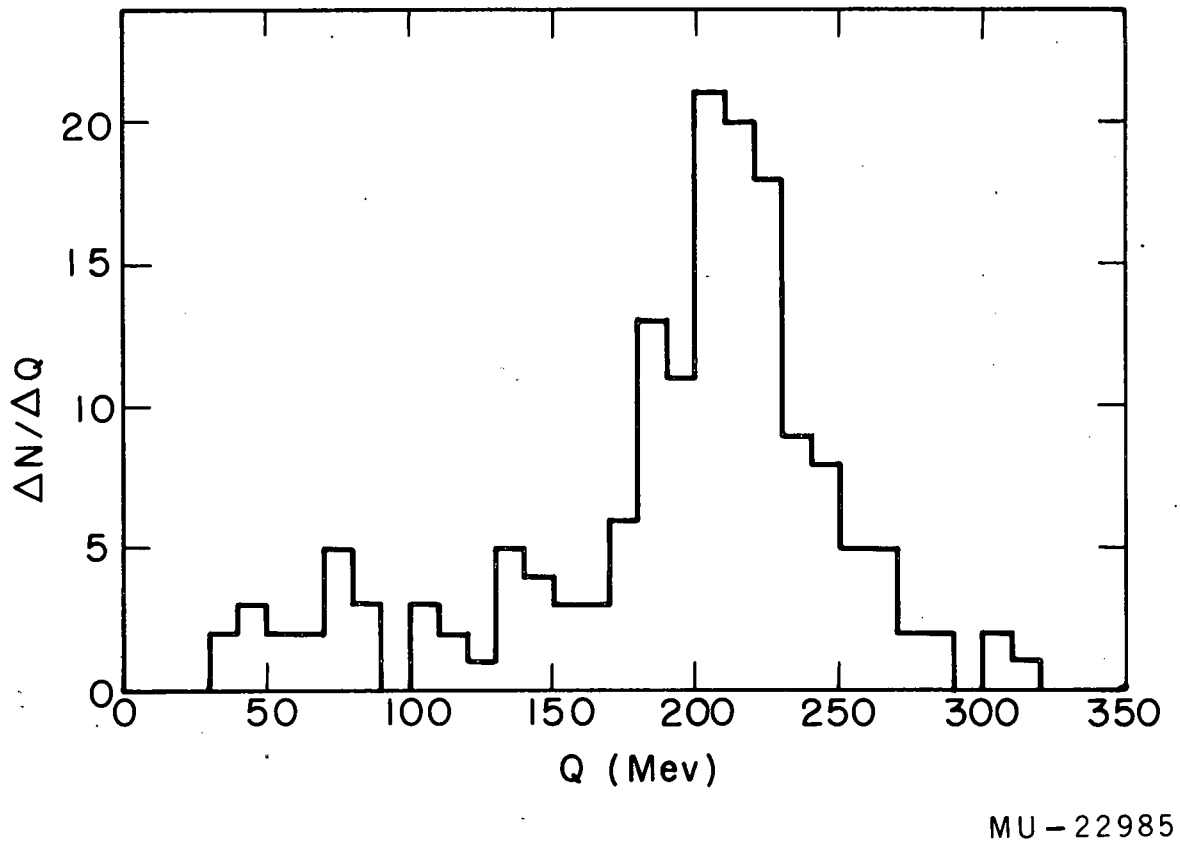

Fig. 13. Q-value distribution of events from the 6-inch plate having P > 500 Mev/c and 0 < t < 2 mean lives.

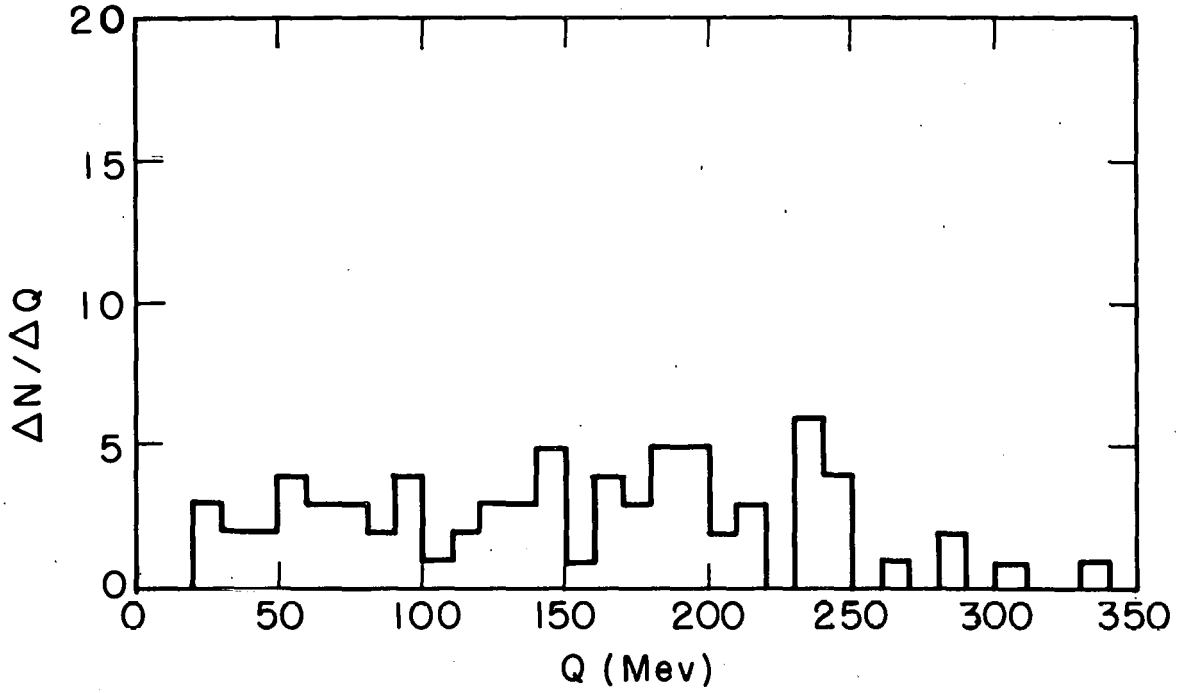

Fig. 14. Q-value distribution of events from the 6-inch plate having P > 500 Mev/c and 2 < t < 4 mean lives.

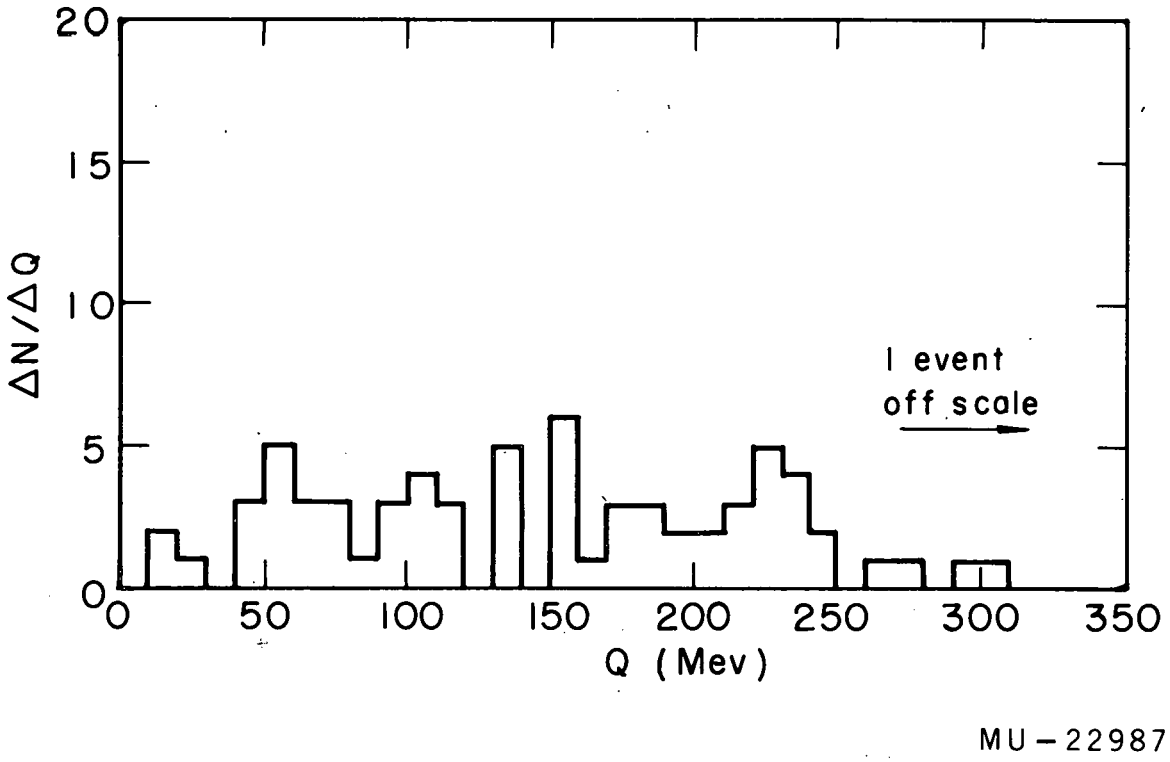

Fig. 15. Q-value distribution of events from the 6-inch plate having P > 500 Mev/c and 4 < t < ∞ mean lives.

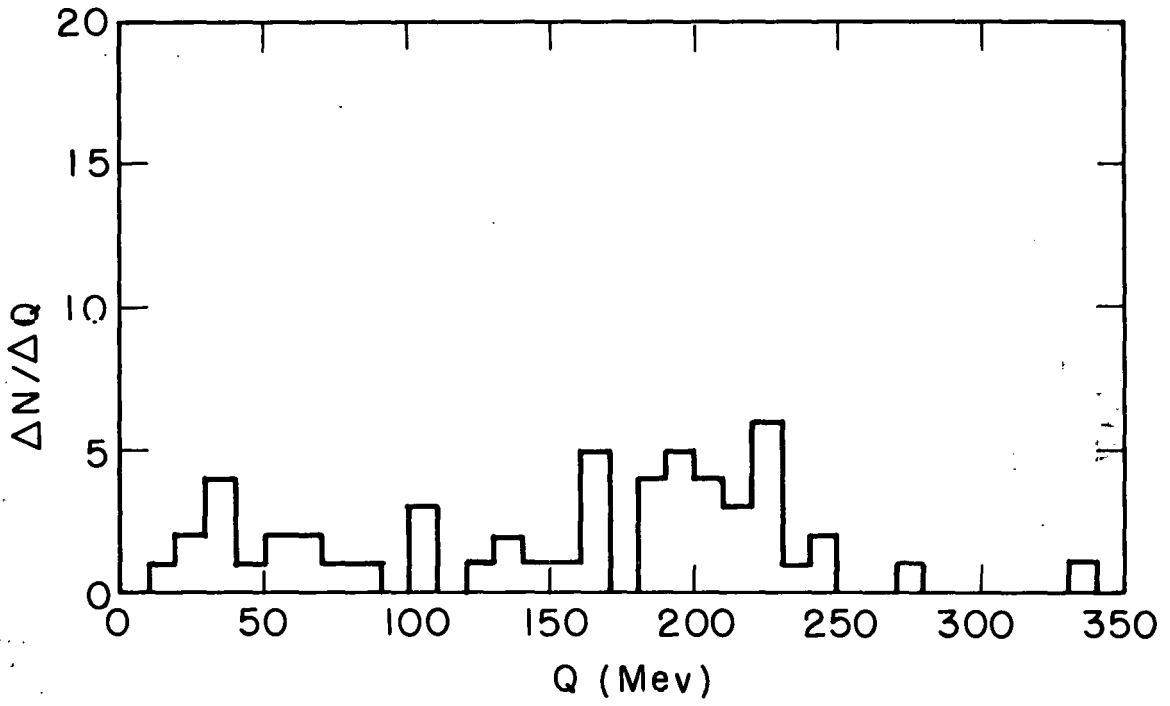

Fig. 16. Q-value distribution of events from the 6-inch plate having P < 500 Mev/c and 0 < t < 2 mean lives.

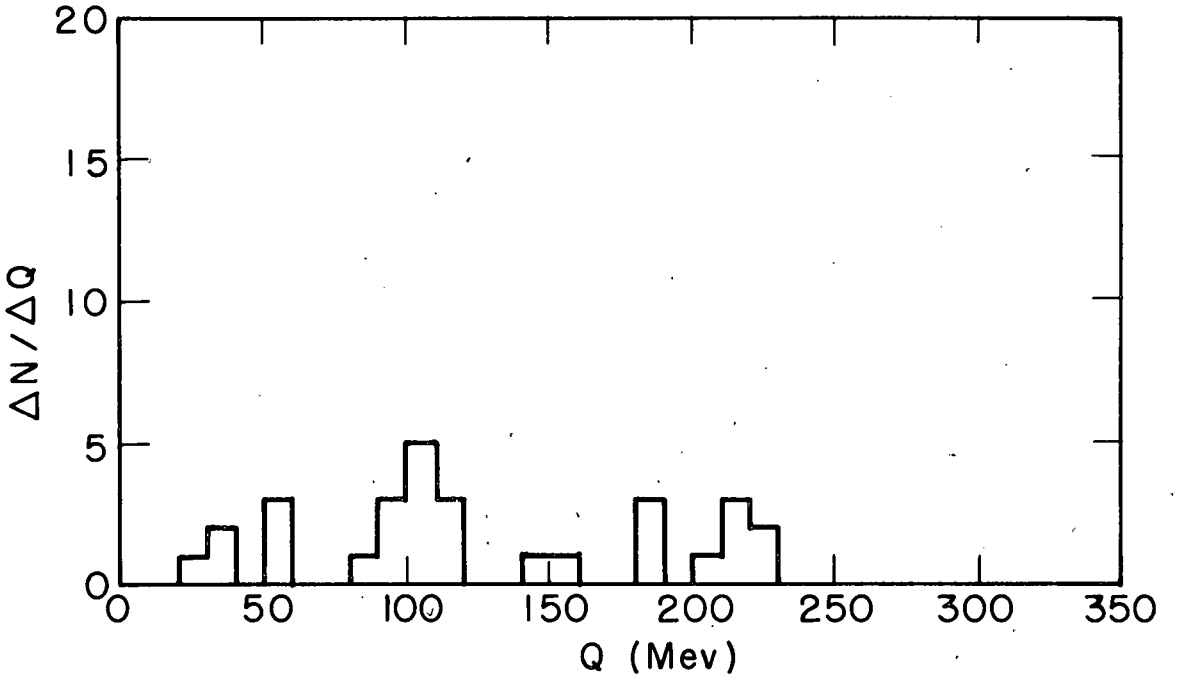

Fig. 17. Q-value distribution of events from the 6-inch plate having $P < 500$ Mev/c and $2 < t_{-} < 4$ mean lives.

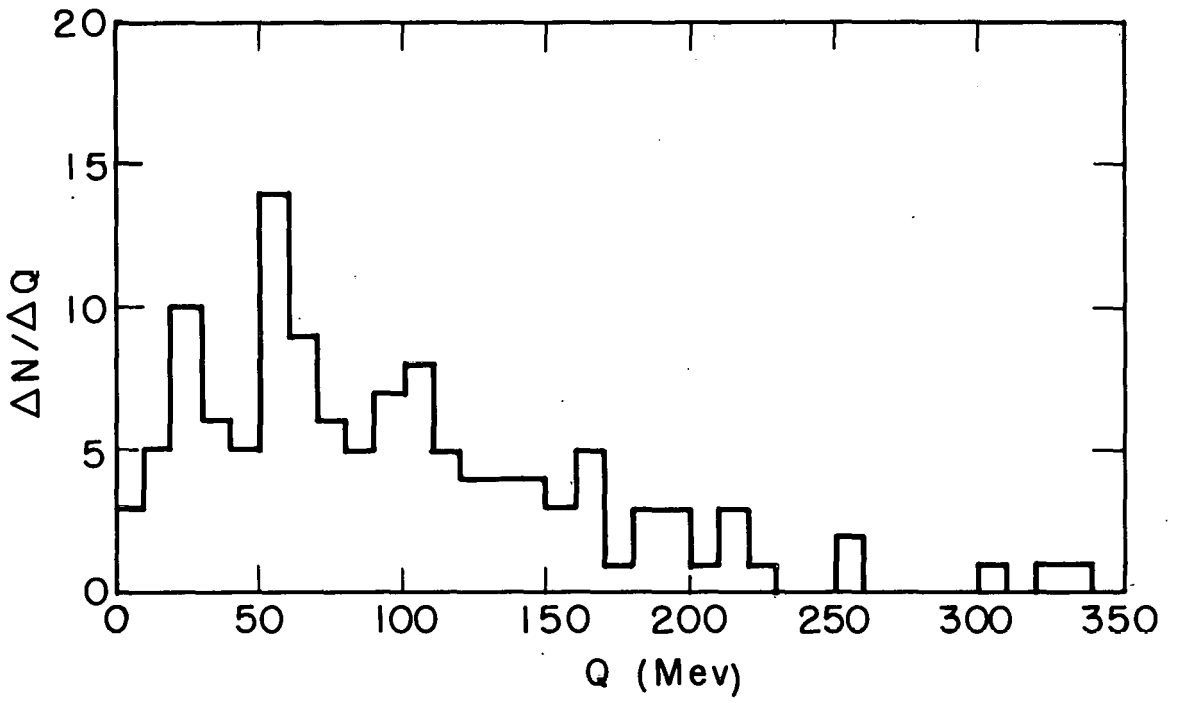

MU-22990

Fig. 18. Q-value distribution of events from the 6-inch plate having P < 500 Mev/c and 4 < t < ∞ mean lives.

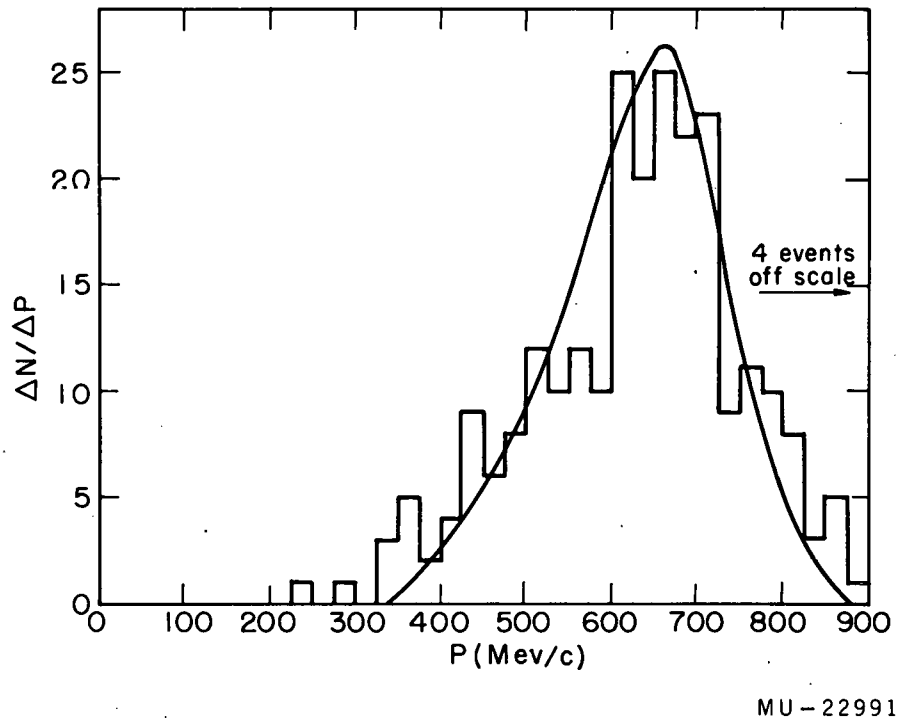

Fig. 19. P distribution of events satisfying the Q and T criteria.

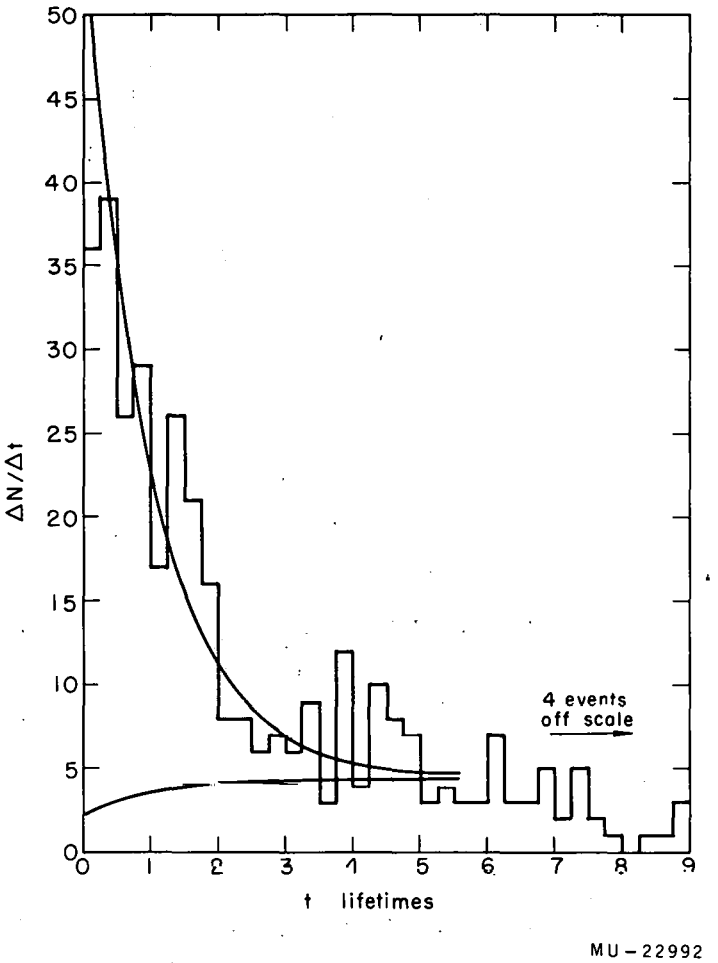

Fig. 20. T distribution of events satisfying the P and Q criteria. Lower curve: background. Upper curve: exponential θ_1 decay plus background.

removes about 13.5% of the θ_1's emerging from the plates. The background of this figure is normalized between two and four mean lives, as described in the following paragraph.

Comparison of Figs. 5, 7, and 13 shows that, of 483 events in the accepted Q region of 170 to 280 Mev, only 210 remain after application of the P and T criteria. Some idea of the background still remaining in this sample of 210 events may be obtained by comparing Figs. 7 and 13 with Figs. 8 and 14. Figures 7 and 13 contain 210 QP-type events for which $0 \leq t < 2$ mean lives, and Figs. 8 and 14 contain 59 QP events for which $2 < t \leq 4$ mean lives. We assume that the background consists of about one-half θ_1's regenerated in propane (see next section) and one-half θ_2 decays and neutron stars. The propane-regenerated θ_1 background is less in the first two mean lives than in the second two, whereas the θ_2-neutron background is about the same. If we call A the number of θ_1's emerging from the metal plate and satisfying the P criterion, and B the constant background per two mean lives at large distances, then we have

$$.865\ A + .784\ B = 210 \text{ events } (0 < t < 2)$$

$$.117\ A + .970\ B = 59 \text{ events } (2 < t < 4)$$

from which

$$A = 211 \text{ and } B = 35.5.$$

Thus in the sample of 210 events there are about 28 background events and 182 θ_1's from the plate.

Adding to 211 the number of θ_1's presumably lost due to the P criterion:

$$\frac{211}{1 - .101} = 235\ \theta_1\text{'s emerging from the plate.}$$

The "signal-to-noise" ratio of θ_1's from the plate to background events is $\frac{235}{248} = .95$ before application of the P and T criteria; afterward it is $\frac{182}{28} = 6.5$. This improvement is obtained with a sacrifice of only 22.2% of the θ_1 mesons available.

The angular distributions of the events satisfying the Q, P, and T criteria are shown in Figs. 21, 22, and 23, along with theoretical curves calculated according to the optical model with $\delta = .8^{30}$ and normalized to the number of events of $\cos\Theta > .970$. The transmission component is assumed to have a Gaussian distribution:

$$\frac{dN}{d\cos\Theta} = A \exp\left(\frac{1-\cos\Theta}{.001}\right)$$

which corresponds to measurement errors of about 2.5°. These curves are consistent with the data, and thus it is clear that both transmission and diffraction regeneration are being observed, in confirmation of the Gell-Mann-Pais particle mixture hypothesis.

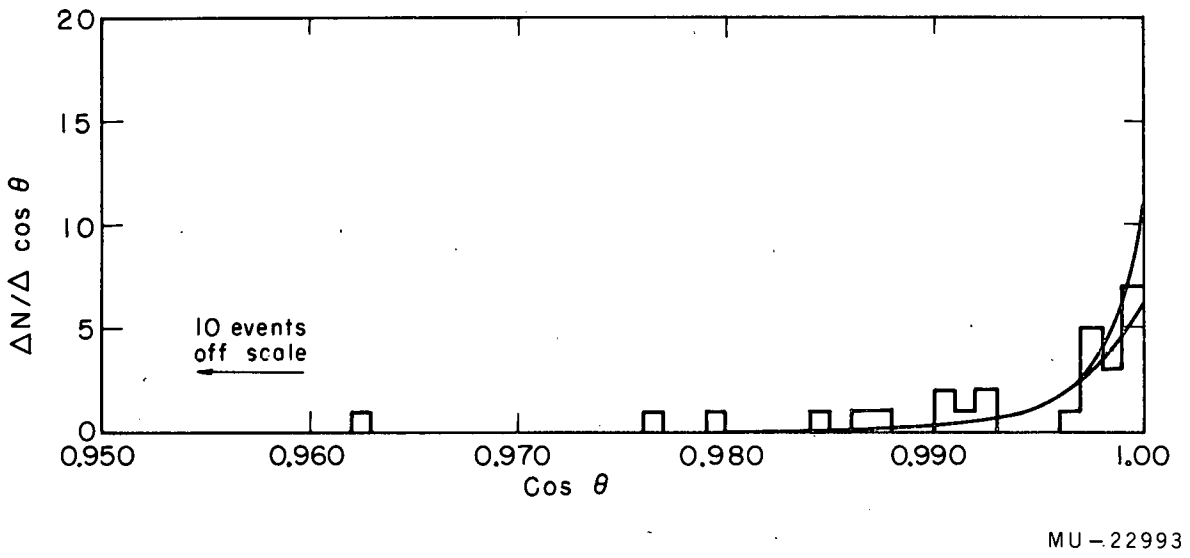

Fig. 21. Angular distribution of events from the 1-1/2-inch lead plate satisfying the Q, P, and T criteria. Lower curve corresponds to nuclear diffraction regeneration. Upper curve includes transmission regeneration.

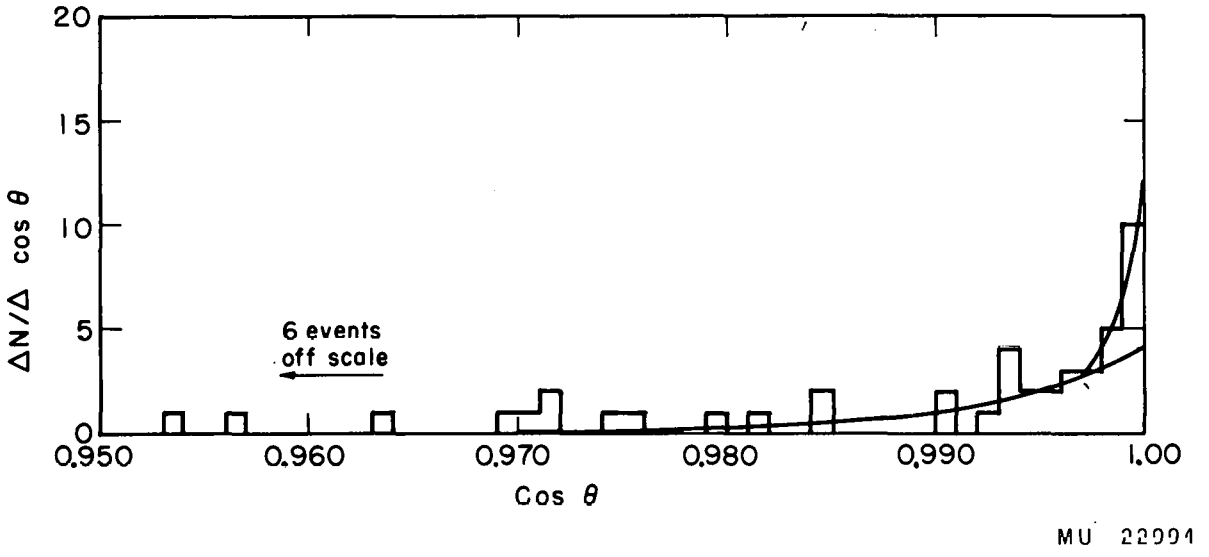

Fig. 22. Angular distribution of events from the 1-1/2-inch iron plate satisfying the Q, P, and T criteria. Lower curve corresponds to nuclear diffraction regeneration. Upper curve includes transmission regeneration.

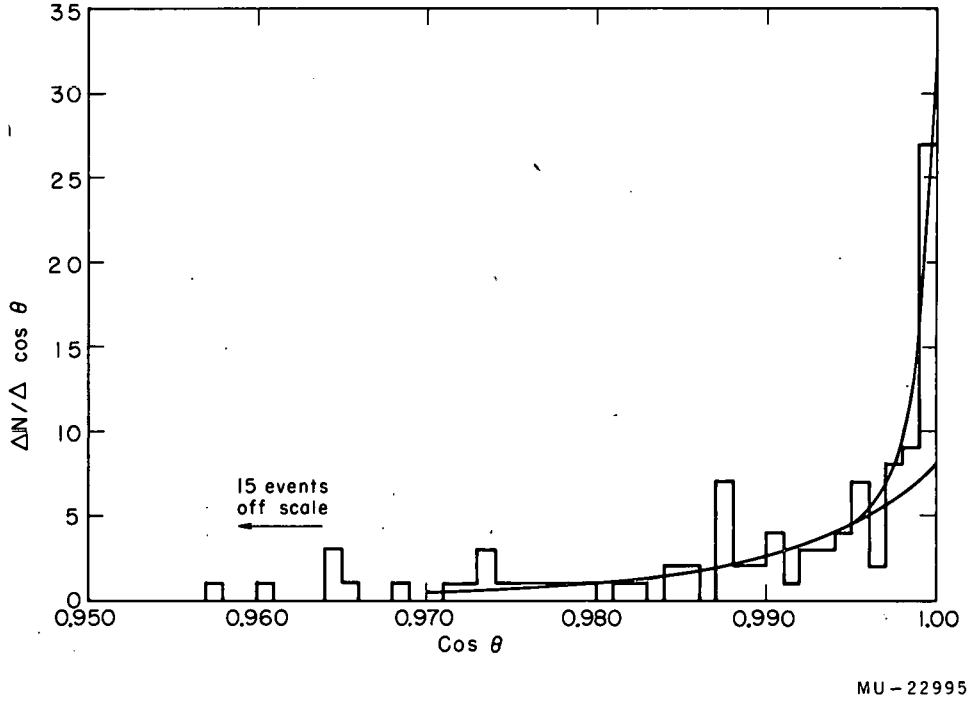

Fig. 23. Angular distribution of events from the 6-inch iron plate satisfying the Q, P, and T criteria. Lower curve corresponds to nuclear diffraction regeneration. Upper curve includes transmission regeneration.

B. Regeneration in Propane.

A search was made for θ_1 regeneration in propane. Using the data of Appendix II, it may be seen that the calculated number of θ_2's traversing the propane of the bubble chamber is

$$1.01 \times 10^5 \ \theta_2 \text{ mesons}$$

for the entire experiment, and the detection efficiency for θ_1's they produce is .28. If the regeneration cross section for carbon is 8.3 mb, as calculated according to the optical model, then one would expect to see 17.3 θ_1's regenerated per mean θ_1 decay length in the propane, without taking into account regeneration on hydrogen and inelastic processes. As these carbon-regenerated θ_1's are masked by the plate-regenerated θ_1's within two mean lives of the plate, and the chamber effectively comes to an end at about seven mean lives from the plate (Fig. 20), one would expect to see about 80 θ_1's in the events occurring more than two mean lives from the plate.

Fig. 24 shows the Q-value distribution of all 324 accepted events satisfying the P criterion and occurring more than two mean lives from the plate, after removal of the expected "residuum" of 28 θ_1's originating in the plate and surviving more than two mean lives. There is no visible θ_1 contribution.

In order to reduce the background, the events occurring in the forward direction have been selected. According to the optical model, 87% of the θ_1's regenerated by diffraction about carbon nuclei should have $\cos\theta > .970$. Fig. 25 shows the Q-value distribution of the events of Fig. 24 that meet the additional requirement $\cos\theta > .970$. The fact that no significant improvement results from this selection indicates that there can be no more than perhaps 50 carbon-regenerated θ_1's in Fig. 24. The success of the optical model calculations in the lead

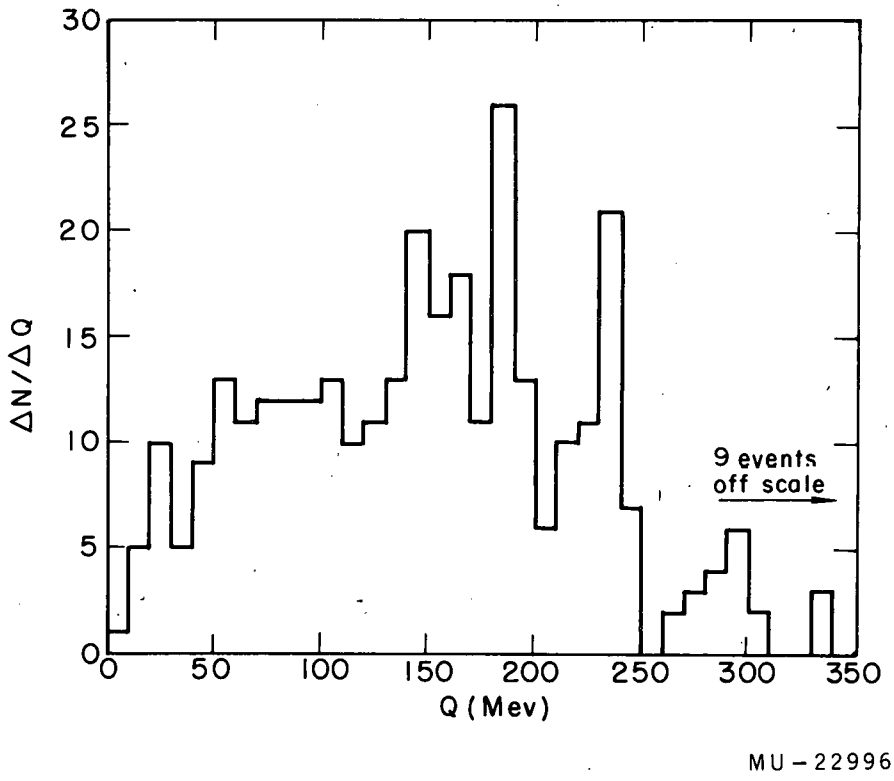

Fig. 24. Q-value distribution of 324 events having P > 500 Mev/c and 2 < t < 00 mean lives, with residuum removed (28 events).

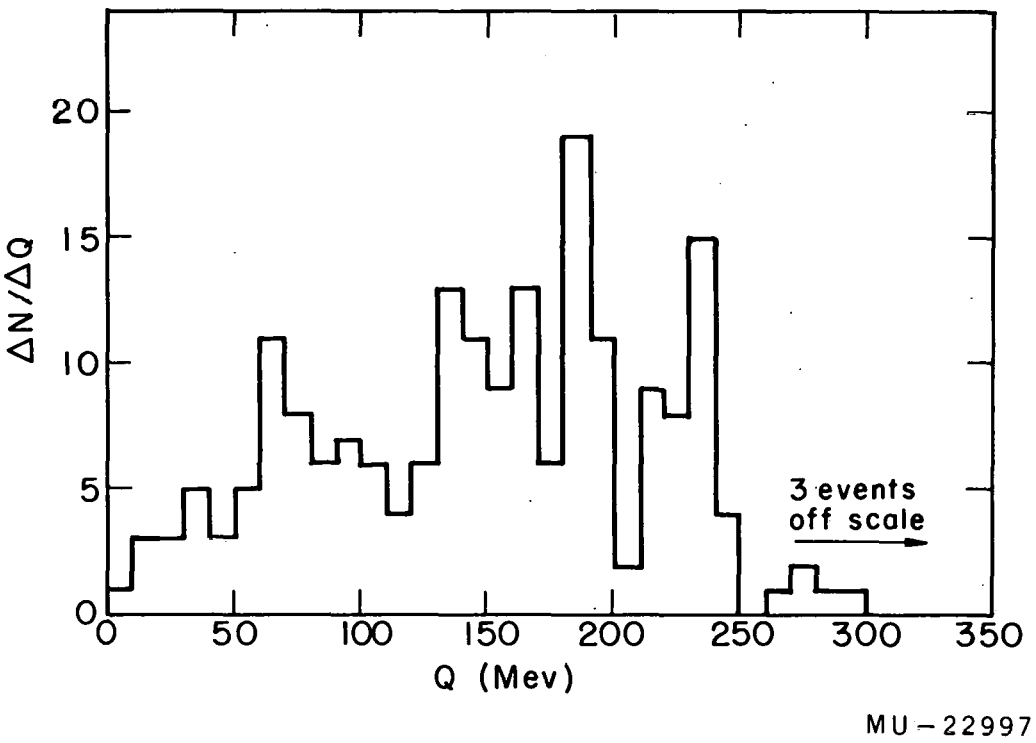

Fig. 25. Q-value distribution of those events of Fig. 24 which have cos $\theta > .970$.

and iron plates, on the other hand, guarantees that there must not be less than 40 or 50 θ_1's regenerated on carbon. Consequently, it seems justifiable to say that approximately half of the events satisfying the Q criterion in Fig. 24 are θ_1's regenerated in propane and half are θ_2 decays and neutron stars.

The angular distribution of the events of Fig. 24 that satisfy the Q criterion is plotted in Fig. 26. A carbon diffraction pattern is included. The figure is not inconsistent with the assumption of θ_1 regeneration to the extent indicated above, but it does not help to demonstrate that regeneration is occurring.

Regeneration on free protons in the propane is more difficult to calculate because of uncertainties not only in the cross sections but also in the angular distributions. However, it is easier to detect because it usually leaves a visible origin, generally a recoil proton, at the point of regeneration. Consequently, almost all of the events that appeared to be θ_1 decays were examined carefully for origins along the reconstructed line of flight within about ten centimeters of the θ_1 decay. Twenty-eight of the origins thus found were subject to a constraint program which required that the event actually satisfy the kinematic conditions for a θ_1 arising in the supposed origin. The program produced a χ^2 value for each event, indicating the probability that the event was consistent with the above hypothesis. These χ^2 values are shown in Fig. 27, along with a theoretical χ^2 curve drawn for three degrees of freedom. On the basis of this figure, twenty events were accepted as true origins, with χ^2 below 15, and eight were discarded.

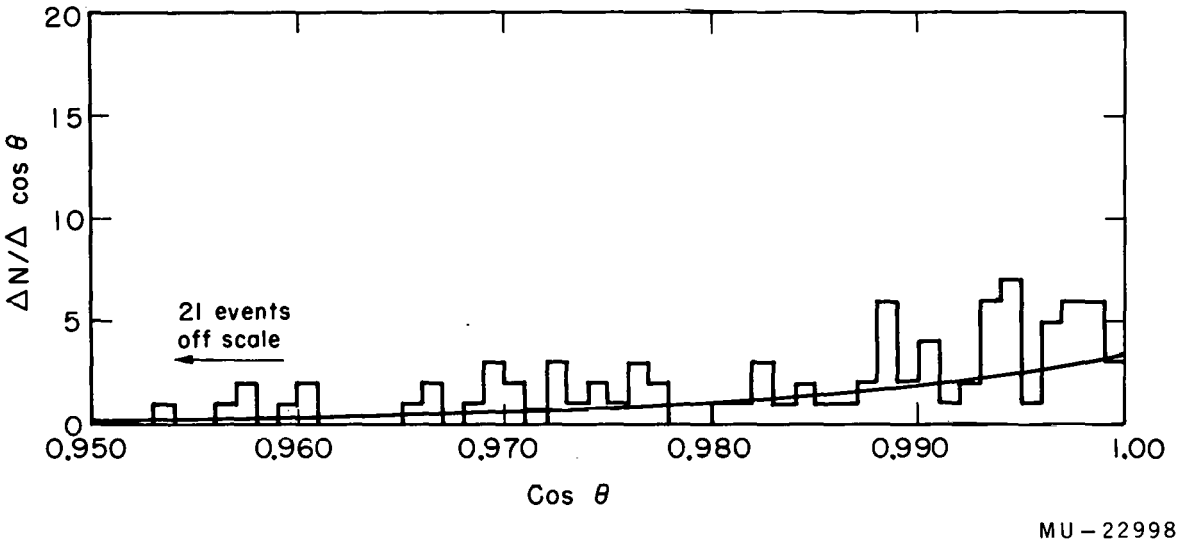

Fig. 26. Angular distribution of the 110 events meeting the Q and P criteria but not the T criterion, with residuum removed (22 events), and carbon diffraction curve normalized to 55 events.

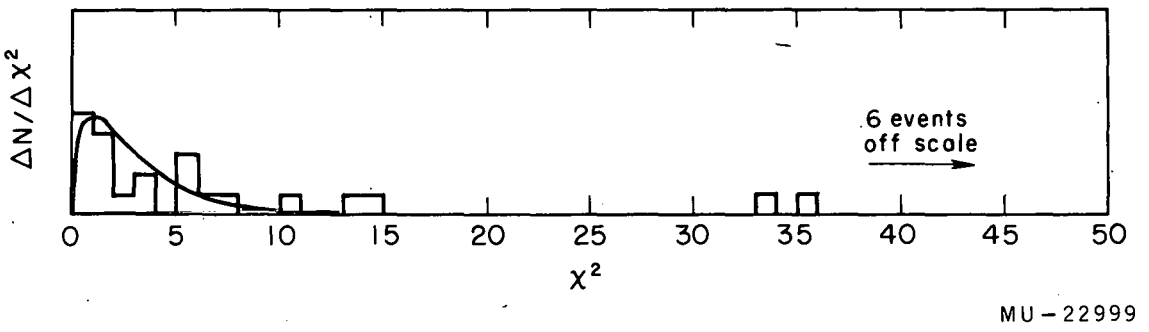

Fig. 27. χ^2 distribution of events with possible origins.

The origins of the regenerated θ_1's should occur more or less uniformly throughout the chamber, as the θ_2 flux does not change appreciably in passing through the propane. Within a few centimeters of the plate, the number of recoil protons due to θ_1-proton scattering may be of the same order of magnitude as the number of θ_1 regeneration origins, because, approximately,

$$\frac{\sigma_{21}}{\sigma_{22}} \sim \frac{1}{100} \quad \text{and} \quad \frac{\text{Number of } \theta_2\text{'s}}{\text{Number of } \theta_1\text{'s}} \sim 100,$$

using σ_{21} for the θ_2-θ_1 regeneration cross section and σ_{22} for the θ_1 elastic scattering cross section, which is the same as the θ_2 elastic scattering cross section. Beyond one or two θ_1 decay lengths from the plate, on the other hand, the number of θ_1 scatters should become negligible. Figure 28 shows the distribution of the distances from the plate to the origins of the θ_1's. The distribution appears to be nearly uniform. Thus this figure suggests that most of the origins are really θ_1 regenerations and that perhaps two or three events, within a few centimeters of the plate, may be due to θ_1 scattering. The θ_1 scatters should of course be indistinguishable from the θ_1 regenerations on the basis of lifetime and angular distribution.

Figure 29 shows the distribution of distances from the plate to the θ_1 decay. The uniform distribution presented here indicates that there are few accidental, false origins, that is, proton recoils or other tracks which accidentally lie along the θ_1 line of flight without actually having taken part in the θ_1's regeneration. Such accidental events occur preferentially near the plate, where the θ_1 density is high. (The slight bunching near the plate observed in Fig. 28 could of course be due to accidental origins of this type.)

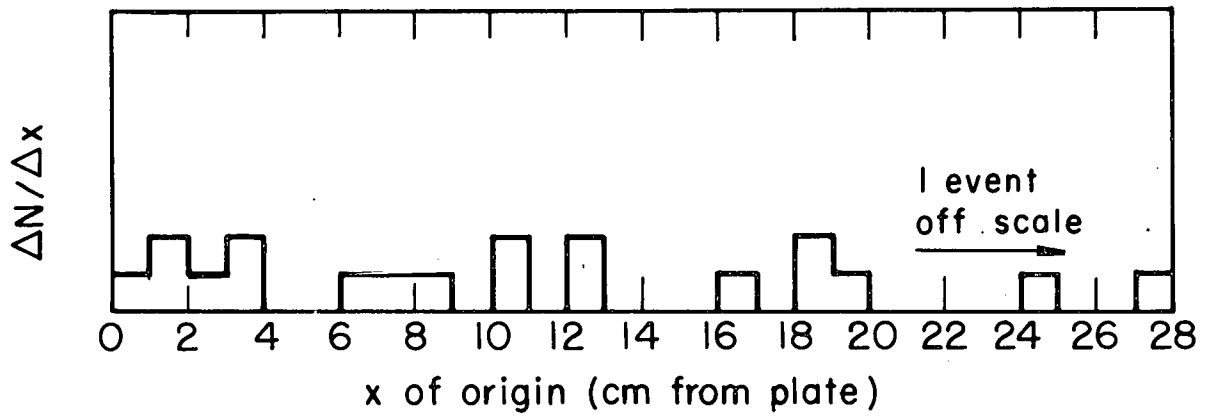

Fig. 28. Distance from plate to origin of θ_1.

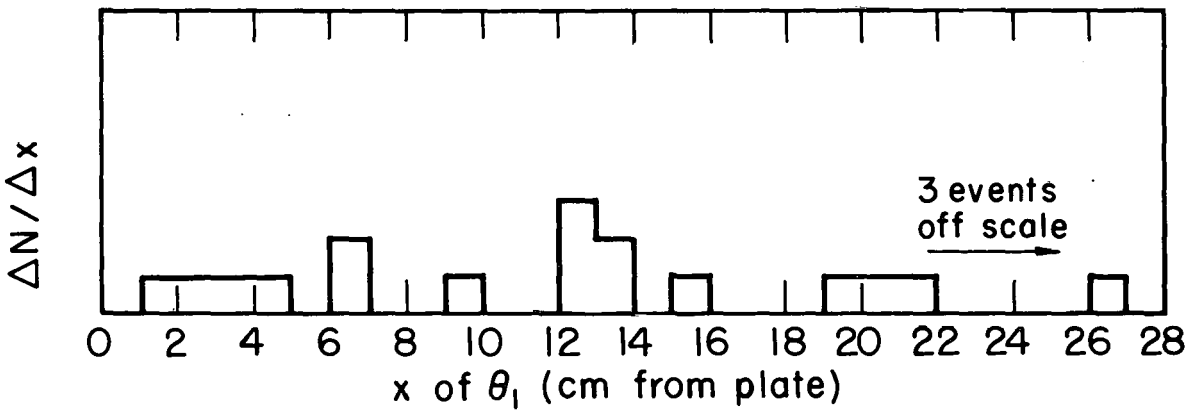

Fig. 29. Distance from plate to θ_1 decay.

The distance from the origin to the θ_1 decay, Fig. 30, on the other hand, should show the exponential decay of the θ_1, whereas the distribution of the background events of high χ^2, Fig. 31, should increase quadratically with distance. The figures are not inconsistent with these predictions, but the number of events is small. If the lifetime of the θ_1 mesons from the origin to the decay is plotted, one obtains Fig. 32. Comparison with the known θ_1 decay curve shows clearly that the θ_1 decays possess the appropriate lifetime and establishes that θ_1 regeneration is indeed being observed.

The angular distribution of the twenty events is shown in Fig. 33. The distribution is wider than the other distributions, Figs. 21, 22, 23, and 26, and is qualitatively what one would expect from regeneration on free protons. This also shows that the θ_1's represented are not a random sample of events from the whole experiment, but rather that these particular events have been regenerated by a process qualitatively different from that involved in regeneration in the plates and in carbon. This further supports the view that the events are not accidental but are examples of θ_1 regeneration on protons.

If one assumes that about half of the protons in the carbon nuclei may be regarded as "free" and equivalent to the protons of the hydrogen of the propane, then one obtains on the basis of these 20 events a value of

$$\sigma_{21} \sim .3 \text{ mb}$$

for free protons.

All of the origins appeared to be proton recoils. The 20 associated events were separated from the other data as they were found,

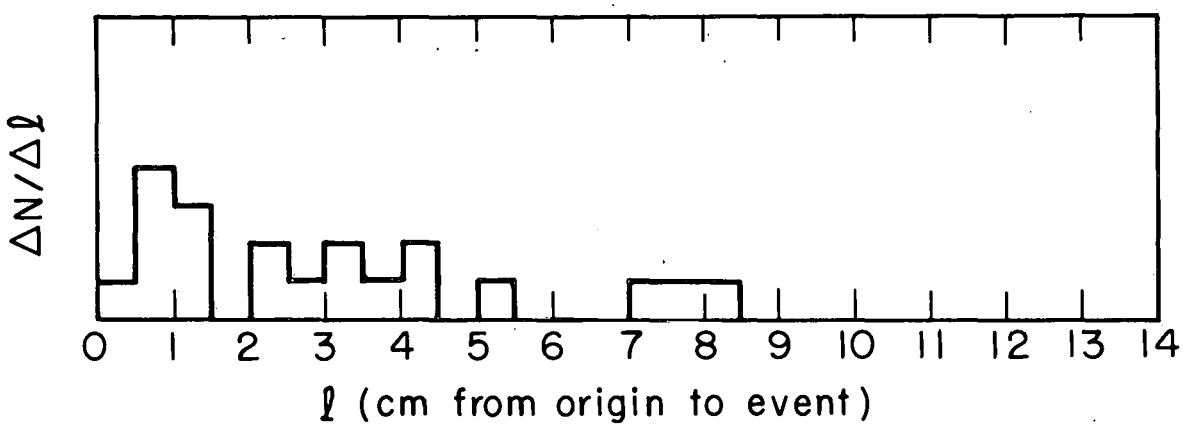

Fig. 30. Distance from origin to θ_1 decay.

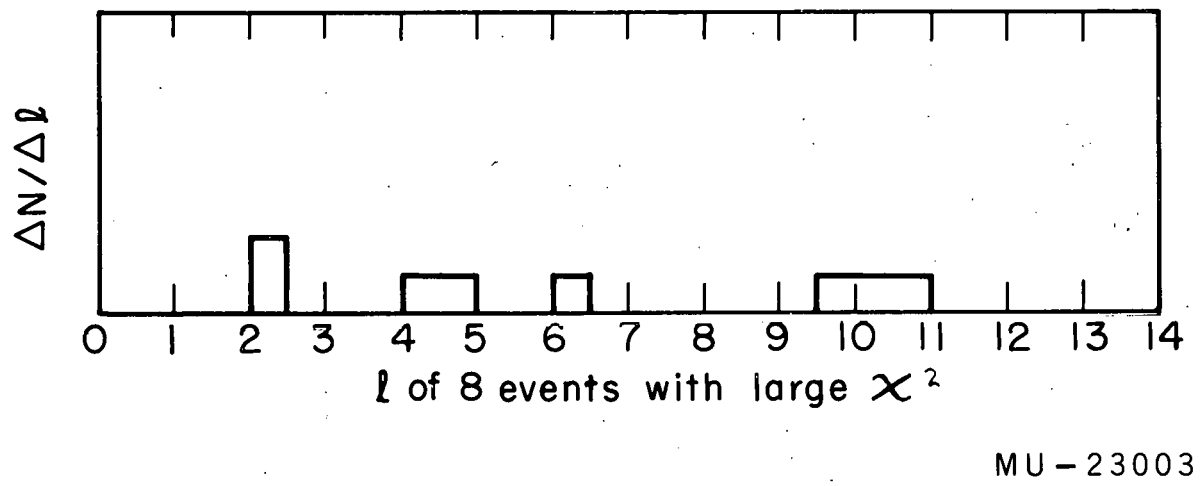

Fig. 31. Distance from false origin to θ_1 decay.

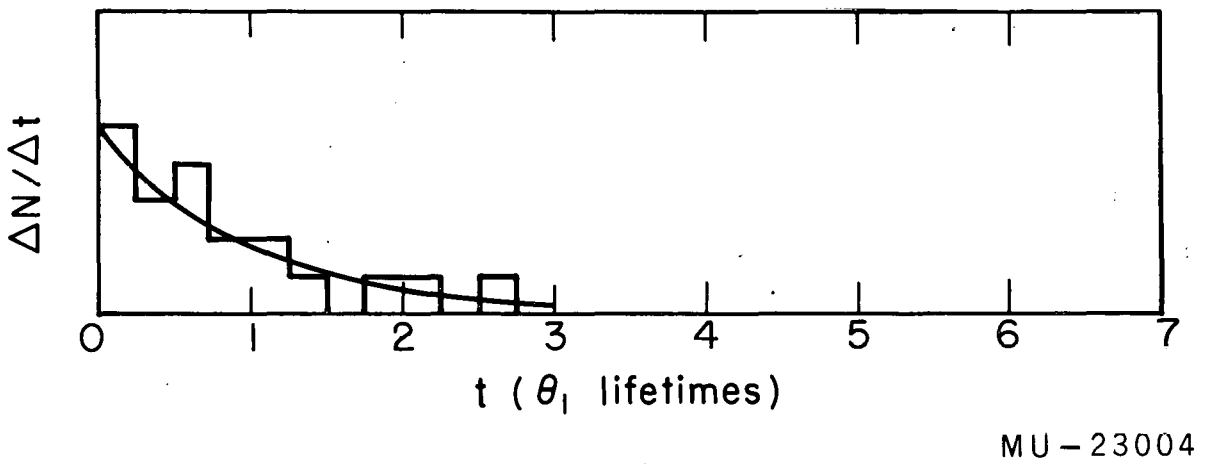

Fig. 32. Lifetime of θ_1 from origin to decay.

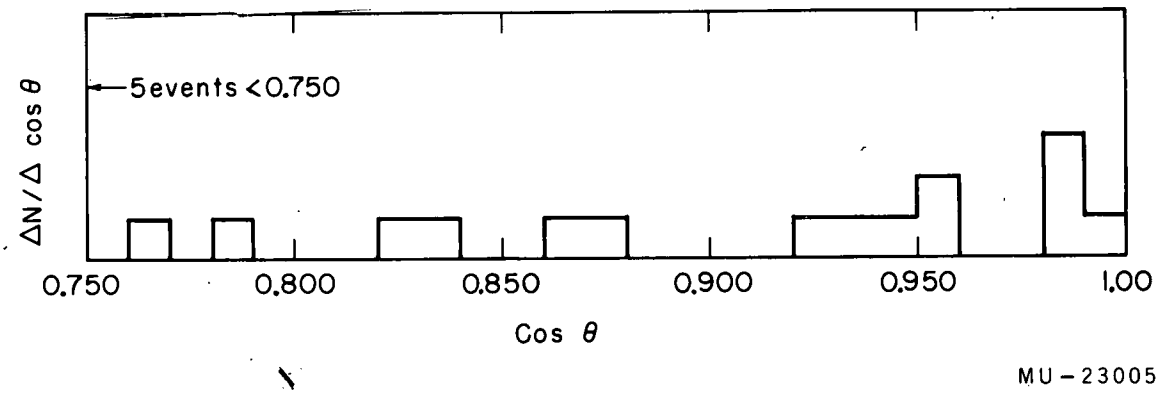

Fig. 33. Angular distribution θ_1's with origins.

and they do not occur on any other histograms in this paper. There are presumably a comparable number of neutron-regenerated $\theta\eta$'s which, of course, could not be identified or separated.

No appreciable transmission regeneration in propane was expected or observed, because of the small total number of regenerated $\theta\eta$'s in the propane.

CONCLUSION

Regeneration of θ_1 mesons from θ_2 mesons has been observed, both in lead and iron plates and in propane, as demonstrated by the Q-value and lifetime of the θ_1 mesons. The θ_1 mesons regenerated in the metal plates showed a characteristic nuclear diffraction pattern and a strong transmission component. These observations further substantiate the Gell-Mann-Pais particle mixture hypothesis. Regeneration by collisions with individual nucleons in propane was detected by means of recoil protons; the diffraction regeneration about carbon nuclei was not detectable above the background.

ACKNOWLEDGEMENTS

The advice, encouragement, and support of Professor Wilson M. Powell are gratefully acknowledged.

Dr. Oreste Piccioni's guidance throughout the experiment was invaluable.

Drs. Francis Muller, William B. Fowler, Robert W. Birge, and Robert P. Matsen made important contributions. Warner Hirsch and Karl Brunstein contributed to the success of the experiment both during the run and in the course of the analysis.

Larry Oswald and many other members of the Cloud Chamber Group ably assisted during the Bevatron run.

Data reduction was handled by Howard White and his staff.

Many other people generously contributed to this experiment, particularly Edward J. Lofgren, Myron L. Good, Richard L. Lander, Robert E. Lanou, Marian N. Whitehead, Roy Kerth, and Frank T. Solmitz. The pictures were scanned by Mrs. Glennette Armeson, Vic Dahmen, Mrs. Roksalana Gamow, Layton Lynch, and Mrs. Ottilie Oldenbusch.

This work was done under the auspices of the U. S. Atomic Energy Commission.

APPENDIX I

Optical Model Calculation

The optical model of the nucleus[22] was used to calculate the diffraction pattern resulting from θ_1 regeneration in iron and lead plates.

If the energy-momentum relationship for a particle outside of a nucleus is written

$$E_o^2 = P_o^2 + M^2$$

where E_o, P_o, and M are the particle's total energy, momentum, and rest mass, respectively, then in the potential V of a nucleus the relationship becomes

$$(E_o + V)^2 = (P_o + \Delta P)^2 + M^2$$

or, if V is small with respect to E_o,

$$\Delta P = - \frac{E_o}{P_o} V$$

or, using $P = \hbar k$,

$$\Delta k = - .00633 \times 10^{13} V$$

since E_o = 835 Mev and P_o = 670 Mev/c for θ_1 mesons in this experiment.

Thus the propagation constant of the particles inside of the nucleus differs from that outside by Δk. Therefore the wave amplitude of a particle which has passed through a nucleus differs from that of a particle which has not by a factor

$$\eta = e^{i \int \Delta k \, dx}$$

where the integral is taken over the path of the particle in the nucleus. The value of Δk varies with nucleon density. If Δk is evaluated at the center of the nucleus, this expression may be replaced by

$$\eta = e^{i \Delta k l(b)}$$

where l(b) is the effective path length in nuclear matter as a function of

b, the impact parameter:

$$l(b) = \frac{1}{\rho_o}\int \rho(r)dx$$

where $\rho(r)$ is the nucleon density as a function of r, the distance from the center of the nucleus.

If a θ_2 wave,

$$\theta_2 = \frac{\theta^o - \bar{\theta}^o}{\sqrt{2}}$$

passes through a nucleus, so that there remains a fraction η of the θ^o and η' of the $\bar{\theta}^o$, then the resultant wave is

$$\frac{\eta\theta^o - \eta'\bar{\theta}^o}{\sqrt{2}} = \frac{\eta - \eta'}{2}\theta_1 + \frac{\eta + \eta'}{2}\theta_2$$

which is equivalent to an undisturbed incident θ_2 wave with a mixture of θ_1 and θ_2 superimposed on it equal to:

$$(\frac{\eta - \eta'}{2})\theta_1 + (\frac{\eta + \eta'}{2} - 1)\theta_2 .$$

This mixture of θ_1 and θ_2 is radiated from the nucleus with a cylindrical-Bessel-function type of angular distribution. The cross sections and scattering amplitudes for processes of interest are then, for a nucleus of radius R:

Diffraction Regeneration:

$$\sigma_{21} = \int_o^R \left|\frac{\eta' - \eta}{2}\right|^2 2\pi b db$$

$$\frac{d\sigma_{21}}{d\Omega} = \left|k\int_o^R \frac{\eta' - \eta}{2} J_o(kb\sin\theta)bdb\right|^2$$

$$f_{21} = ik\int_o^R \frac{\eta' - \eta}{2} J_o(kb\sin\theta)bdb$$

Elastic Scattering:

$$\sigma_{22} = \int_o^R \left|1 - \frac{\eta' + \eta}{2}\right|^2 2\pi b db$$

$$f_{22} = ik\int_o^R (1 - \frac{\eta' + \eta}{2}) J_o(kb\sin\theta)bdb$$

Inelastic Scattering:

$$\sigma_{in} = \int_0^R (1 - \left| \frac{\eta' + \eta}{2} \right|^2) 2\pi b db$$

These quantities have been evaluated by numerical integration (see Table II). A trapezoidal nuclear density distribution was employed:

$$\rho(r) = \rho_t \left(\frac{R - r}{R - r_o}\right) \quad \text{for} \quad r_o < r < R$$
$$= \rho_t \quad \text{for} \quad 0 < r < r_o$$

For this model, the effective path length in nuclear matter is:

$$l(b) = \frac{1}{R - r_o}\left(R\sqrt{R^2 - b^2} - r_o\sqrt{r_o^2 - b^2} - b^2 \ln\frac{R + \sqrt{R^2 - b^2}}{r_o + \sqrt{r_o^2 - b^2}}\right)$$
$$\text{for } 0 < b < r_o,$$

$$= \frac{1}{R - r_o}\left(R\sqrt{R^2 - b^2} - b^2 \ln\frac{R + \sqrt{R^2 - b^2}}{b}\right) \text{ for } r_o < b < R.$$

Values of r_o, R, and ρ_t deduced from the data of Hofstadter[37] are presented in Table II.

For θ^o cross section that of the K^+ meson was used, and for $\bar{\theta}^o$ cross section that of the K^- meson was used (see Introduction). For K^+ energies corresponding to those of this experiment, Zorn and Zorn[38] find K^+-nucleon total cross sections of about 15 mb and give the following nuclear potentials:

K^+ Momentum	Real Potential	Imaginary Potential
568 Mev/c	18.5 ± 3.6 Mev	- 17.4 ± 2.0 Mev
656 Mev/c	13.5 ± 5.0 Mev	- 17.6 ± 2.5 Mev

These potentials are proportional to the density of nuclear matter, and so they must be corrected for the difference between the nuclear density distribution used by Zorn and Zorn and that of the trapezoidal model.

TABLE II

	Carbon	Iron	Lead
R, fermis	3.5	5.5	7.7
r_o, fermis	1.2	2.7	5.2
ρ_t, nucleons/fermi^3	.178	.172	.178
ρ_z, nucleons/fermi^3	.107	.135	.147
σ_{21}, mb	8.3	25.8	41.6
σ_{22}, mb	51.3	289	996
σ_{in}, mb	177	597	1510
f^o_{21}, fermis	-2.24-1.39i	-6.70-3.85i	-12.6-6.1i
f^o_{22}, fermis	0.28+6.18i	1.62+24.0i	4.63+65.8i
a^2	.020	.007	.003

Zorn and Zorn use the density distribution:

$$\rho(r) = \rho_z(1 + \exp \frac{r - r_o}{d})^{-1}$$

with d = .57 fermi and $r_o = 1.15\ A^{1/3}$ fermi. This yields a density at the center of the nucleus of:

$$\rho_z = \left[\frac{4}{3}\pi r_o^3 \left(1 + \frac{\pi^2 d^2}{r_o^2}\right)\frac{1}{A}\right]^{-1}$$

(See Table II.) For iron the ratio of the trapezoidal ρ_t to the Zorn and Zorn ρ_z is 1.27. The corrected θ^o potentials are then:

θ^o Momentum	V
568 Mev/c	23.5 - 22.1 i Mev
656 Mev/c	17.2 - 22.3 i Mev

The densities, and therefore the potentials, are assumed to be the same for lead and carbon nuclei as for iron nuclei.

According to the data of Chamberlain et al.[39], the total K^--p cross section at 670 Mev/c is 40 mb, and the K^--n cross section is 28 mb. We have therefore used an average K^--nucleon cross section of 33.6 mb. The exponential decrease in the K^- wave amplitude upon crossing the nucleus may be expressed approximately by

$$\eta = \exp -\frac{\sigma_t \rho_t l(b)}{2} = \exp \mathrm{Re}(i\Delta k l(b)) = \exp \mathrm{Re}\left(-i\frac{E_o}{\hbar c P_o c} V l(b)\right)$$

which yields Im V = - 45.5 Mev. The real part of the K^- potential has not been determined, but it may be approximately equal and opposite to that of the K^+ [40]. We have assumed therefore the following potentials for the $\overline{\theta^o}$ meson in nuclear matter:

$$V = - 19 - 45.5\ i \text{ Mev.}$$

As the regeneration cross sections are sensitive to the real $\overline{\theta^o}$ potential, calculations based on the highly uncertain value given above

cannot be expected to give the number of θ_1's regenerated to within a factor of less than two. The angular distributions, on the other hand, are relatively independent of potentials, and depend almost entirely on the size of the nucleus, the θ_1-θ_2 mass difference and the thickness of the plate.

The above treatment corresponds to single scattering from nuclei. Formulas for multiple scattering have been developed by Matsen,[32] using Gaussian approximations to the angular distributions (see Table II):

$$d\sigma/d\Omega(\theta) \approx d\sigma/d\Omega(0)\ \exp(1 - \cos\theta)/a^2$$

The results are too complicated to be given here. The angular distributions of Figs. 21, 22, and 23 include multiple scattering effects.

APPENDIX II

Expected Number of Θ_1's

The Bevatron beam level was generally between 5×10^{10} and 10^{11} protons per pulse, which yielded between 10^6 and 2×10^6 pion counts per pulse. The total number of protons striking the Bevatron target was:

4.8×10^{15} protons, for the 1⅓-inch lead and iron plate

7.2×10^{15} protons, for the 6-inch iron plate

These figures were established by monitoring the internal proton beam of the Bevatron; in portions of the experiment in which such monitoring was not complete, values were interpolated by means of counting frequency of occurrence of certain types of tracks in the bubble chamber.

Scintillation counters were employed to establish the number of pions negotiating the experimental channel per proton striking the target. The number, which includes a correction of approximately 20% due to contamination of the pions with muons (5%) and electrons (15%), is:

One pion per 6×10^4 protons.

The pions, of momentum 1.1 Bev/c (± 5%), struck a liquid hydrogen target which was 60 inches long. At 276 inches beyond the center of this target lay the regenerating plate of the propane bubble chamber, which was 4 inches high and 14½ inches wide and thus subtended a solid angle of 7.6×10^{-4} steradian. Using the following values:

0.42×10^{23} protons/cm^3 in liquid hydrogen

0.15 mb/ster for $\Lambda^0\Theta^0$ production
0.05 mb/ster for $\Sigma^0\Theta^0$ production

6.5 relativistic solid-angle contraction in laboratory frame,

we find 6.3×10^{-6} Θ^0 per pion, which is 1.05×10^{-10} Θ^0 per proton.

Of the θ^0's produced in the hydrogen target, the fraction surving various hazards is:

.50 θ_1 decay
.92 Interactions in hydrogen target
.47 Four-inch lead window
.95 Collimator
.85 Two-inch iron wall of bubble chamber, with thin window
.76 θ_2 decay

.133 θ_2 survival to plate inside bubble chamber;

and for θ_1's emerging from the plate inside the bubble chamber:

.67 Charged decay
.89 Scanning efficiency
.70 Poor (unmeasurable) events
.75 Q, P, and T criteria
.80 P_2 less than 600 Mev/c

.250 Detection effieiency

The number of θ_1 mesons regenerated by diffraction and transmission on the various plates per incident θ_2 meson has been estimated by Matsen[32] taking into account multiple scattering and the θ_1-θ_2 mass difference. As this number is sensitive to the K^- nuclear potential, which is at present unknown, the result could be in error by as much as 50% (see Appendix I). The error accumulated in the long series of effects included in the calculation of the number of θ^0's produced, the survival fraction, and the detection efficiency, amounts to about 30%. Table III shows the number of θ_1's thus calculated, compared to the number found experimentally. Considering the errors involved, the excellent agreement in total number of θ_1's regenerated must be regarded as somewhat fortuitous. The agreement in relative contributions of the various plates, on the other hand, is to be expected if the optical model has any validity for these purposes.

TABLE III

	1½-Inch Lead	1½-Inch Iron	6-Inch Iron
Θ_2's incident on plate	$.333 \times 10^5$	$.333 \times 10^5$	1.00×10^5
Estimated Θ_1's per Θ_2	.00296	.00468	.00436
Total Θ_1 expected	25	39	109
Θ_1 found experimentally ($\cos \theta > .970$)	26	40	96
Θ_2 fraction surviving plate	.828	.825	.464

BIBLIOGRAPHY

1. For the historical development of the subject see J. G. Wilson and S. A. Wouthuysen, Progress in Elementary Particle and Cosmic Ray Physics, (North Holland Publishing Co., Amsterdam, 1958), Vol. IV, pp 71-103.

2. G. D. Rochester and C. C. Butler, Nature, 160, 855 (1947).

3. C. M. G. Lattes, G. P. S. Occhialini, and C. F. Powell, Nature, 160, 453 (1947).

4. R. W. Thompson, A. V. Buskirk, L. R. Etter, C. J. Karzmark, and R. H. Rediker, Phys. Rev. 90, 1122 (1953).

5. J. G. Wilson, Progress in Cosmic Ray Physics, (North Holland Publishing Co., Amsterdam, 1956), Vol. III, pp 310-321.

6. Arthur Roberts, Proceedings of the Rochester Conference on Meson Physics (January, 1952), Appendix IV: Summary of Proceedings.

7. C. S. Wu, E. Ambler, R. W. Hayward, D. D. Hoppes, and R. P. Hudson, Phys. Rev. 105, 1413 (1957).
R. L. Garwin, L. M. Lederman, and M. Weinrich, Phys. Rev. 105, 1415 (1957).
J. I. Friedman and V. L. Telegdi, Phys. Rev. 105, 1681 (1957).

8. T. D. Lee and C. N. Yang, Phys. Rev. 104, 254 (1956).

9. W. K. H. Panofski, L. L. Fitch, R. M. Motley, and W. G. Chestnut, Phys. Rev. 109, 1353 (1958).

10. U. Camerini, W. F. Fry, M. Baldo-Ceolin, H. Huzita, and S. Natali, Phys. Rev. 115, 1048 (1959).

11. A. Pais, Phys. Rev. 112, 624 (1958).

12. Murray Gell-Mann, Phys. Rev. 92, 833 (1953).
T. Nakano and K. Nishijima, Progr. Theoret. Phys. (Kyoto), 10, 581 (1953).

13. M. Gell-Mann and A. Pais, Phys. Rev. 97, 1387 (1955).
R. Gatto, Phys. Rev. 106, 168, (1957).
T. D. Lee, R. Oehme, and C. N. Yang, Phys. Rev. 106, 340 (1957).

14. M. Gell-Mann and A. H. Rosenfeld, Ann. Rev. Nuclear Sci. 7, 407 (1957).
F. S. Crawford, Jr., M. Cresti, R. L. Douglass, M. L. Good, G. R. Kalbfleisch, and M. L. Stevenson, Phys. Rev. Letters 2, 361 (1959).

15. K. Lande, L. M. Lederman, and W. Chinowsky, Phys. Rev. 105, 1925 (1957).

16. E. Eisler, R. Plano, N. Samios, M. Schwartz, and J. Steinberger, Nuovo cimento 5, 1700 (1957).

17. W. B. Fowler, R. L. Lander, andW. M. Powell, Phys. Rev. 113, 928 (1959).
F. S. Crawford, Jr., M. Cresti, M. L. Good, K. Gottstein, E. M. Lyman, F. T. Solmitz, M. L. Stevenson, and H. Ticho, Phys. Rev. 113, 1601 (1959).

18. R. Ammar, J. I. Friedman, R. Levi Setti, and L. I. Telegdi, Nuovo cimento 5, 1801 (1957).
M. Baldo-Ceolin, C. C. Dilworth, W. F. Fry, W. D. B. Greening, H. Huzita, S. Limentani, and A. E. Sicherollo, Nuovo cimento 6, 130 (1957).
M. Baldo-Ceolin, H. Huzita, S. Natali, U. Camerini, and W. F. Fry, Phys. Rev. 112, 2118 (1958).
V. Bisi, R. Cester, A. Debenedetti, C. M. Garelli, N. Margem, B. Quassiati, and M. Vigone, Nuovo cimento 12, 16 (1959).

19. D. R. Inglis, Revs. Modern Phys. 33, 1 (1961).

20. W. H. Barkas and A. H. Rosenfeld, Proceedings of the 1960 International Conference on High Energy Physics at Rochester(Interscience Publishers, Inc., 1960), p 877.

21. A. Pais and O. Piccioni, Phys. Rev. 100, 1487 (1955).
F. Muller, R. W. Birge, W. B. Fowler, R. H. Good, W. Hirsch, R. P. Matsen, L. Oswald, W. M. Powell, H. S. White, and O. Piccioni, Phys. Rev. Letters 4, 418 (1960).

22. S. Fernbach, R. Serber, and T. B. Taylor, Phys. Rev. 75, 1352 (1949).

23. K.Aizu, Nuovo cimento 6, 1040 (1957).

24. W. F. Fry and R. G. Sachs, Phys. Rev. 109, 2212 (1958).

25. E. Boldt, D. O. Caldwell, and Y. Pal, Phys. Rev. Letters 1, 150 (1958).

26. R. W. Birge, R. P. Ely, W. M. Powell, H. Huzita, W. F. Fry, J. A. Gaides, S. Natali, R. B. Willman, and U. Camerini, Proceedings of the 1960 International Conference on High Energy Physics at Rochester (Interscience Publishers, Inc., 1960), p 601.
W. F. Fry, private communication.

27. S. B. Trieman andR. G. Sachs, Phys. Rev. 103, 1545 (1956).
Ya. B. Zel'dovich, J. Exptl. Theoret. Phys. (U.S.S.R.) 30, 1168 (1956) (Translation: Soviet Phys.--JETP 3, 989 (1957)).

28. N. Biswas, Phys. Rev. 118, 866 (1960).

29. S. B. Trieman and S. Weinberg, Phys. Rev. 116, 239 (1959).

30. I. Yu. Kobzarev and L. B. Okun', J. Exptl. Theoret. Phys. (U.S.S.R.) 39, 605 (1960) (Translation: Soviet Phys.--JETP, to be published).

31. K. M. Case, Phys. Rev. 103, 1449 (1956).
M. L. Good, Phys. Rev. 106, 591 (1957).
M. L. Good, Phys. Rev. 110, 550 (1958).
Ya. B. Zel'dovich, J. Exptl. Theoret. Phys. (U.S.S.R.) 36 1381 (1959) (Translation: Soviet Phys.--JETP 36(9), 984(1959)).

32. R. P. Matsen, thesis (unpublished).

33. M. Lax, Revs. Modern Phys. 23, 287 (1951), especially page 290.

34. We are indebted to Vic Brady of Lawrence Radiation Laboratory for carrying out these calculations.

35. R. H. Good and O. Piccioni, Rev. Sci. Instr. 31, 1035 (1960).

36. W. M. Powell, W. B. Fowler, and L. Oswald, Rev. Sci. Instr. 29, 874 (1958).

37. R. Hofstadter, Revs. Modern Phys. 28, 214 (1956).

38. B. Sechi-Zorn and G. T. Zorn, Phys. Rev. (to be published).

39. O. Chamberlain, K. M. Crowe, D. Keefe, L. T. Kerth, A. Lemonick, T. Maung, and T. F. Zipf (to be published).

40. See, for example, Proceedings of the 1960 International Conference on High Energy Physics at Rochester (Interscience publishers, Inc., 1960), pp 487, 493.